



Andrés L. Suárez González, BSc.

# User Interface to compare force and power in the machining process

MASTER THESIS

For obtaining the academic degree

Diplom-Ingenieur

Master Program of Production Science and Management

Graz University of Technology

Supervisor:

Univ.-Prof. Dipl.-Ing. Dr.techn. Franz Haas

Faculty of Mechanical Engineering,

Graz, September 2016

## EIDESSTATTLICHE ERKLÄRUNG

Ich erkläre an Eides statt, dass ich die vorliegende Arbeit selbstständig verfasst, andere als die angegebenen Quellen nicht benutzt und die den benutzten Quellen wörtlich und inhaltlich entnommenen Stellen als solche gekennzeichnet habe.

*I declare that I have authored this thesis independently, that I have not used other than the declared sources/resources, and that I have explicitly indicated all material which has been quoted either literally or by content from the sources used.*

---

(Datum/Date)

---

(Unterschrift/ Signature)

## Abstract

Within the framework of the Industry 4.0, it is stated that digital technologies have the capacity to transform the way of manufacturing. Machines nowadays include a myriad of sensors, actuators, and tools that increase the amount of available data of the process or the connectivity between the user and the device. Companies should then find and analyze the right data in order to take decisions that will thus positively define business performance. Summarized, to “move from big data to smart data”.

This thesis represents one step done at the Graz University of Technology and in particular at the Institute of Production Engineering to implement digital tools in pursuance of a proper evaluation of machining processes. The thesis deals with an evaluation software that allows the comparison of the influence of power and force in the machining process and that also finds the differences between processes with dissimilar characteristics like cutting depth or feed rate. It could also be used for machine comparisons, concerning energy consumption when grinding, milling or turning.

The software can be used for a basic evaluation of the implementation of Ultrasonic Assisted Machining (UAM) and then to compare it with a traditional machining process. The results should be able to show the advantages of the ultrasonic technology in the area of machining processes. The practical implementation of the software will give a hint to find further investigations of how the machining process can be positively improved.

## Kurzfassung

Im Rahmen der Industrie 4.0 steht die Digitalisierung im Zentrum. Heutzutage sind die Maschinen mit einer Vielzahl an Sensoren, Antrieben und Werkzeugen ausgestattet, die die anfallende Datenmenge eines Prozesses erheblich erhöhen können. In diesem Fall sollen Unternehmen einen Weg finden, die Sensordaten der Maschinen zu analysieren, damit richtige Strategien verfolgt werden können. Das Ziel soll sein, das große Datenvolumen zu smarten Informationen zu verdichten.

Die hier vorgelegte Masterarbeit, ausgehend vom Institut für Fertigungstechnik der Technischen Universität Graz insbesondere dem, stellt einen Entwicklungsschritt in die beschriebene Richtung dar. Im Fokus liegt die Entwicklung einer Software, mit der man den Einfluss von Kraft und Leistung vergleichen kann und Unterschiede zwischen zwei oder mehreren Fertigungsprozessen, bei Änderungen der Prozessparameter während des Bearbeitungsverfahrens aufdecken kann.

Die Software kann auch für eine Bewertung der Ultrasonic-Technologie während der Zerspanung angewendet werden, um dann mit einem üblichen Bearbeitungsverfahren verglichen zu werden. Die Ergebnisse werden nicht nur die Vorteile der neuen Technologie aufzeigen, sondern auch die praktische Anwendung der Software, damit weitere Untersuchungen zur Verbesserung der Fertigungsprozesse entwickelt werden können.

Table of Content	
<b>EIDESSTATTLICHE ERKLÄRUNG</b> .....	<b>ii</b>
<b>Abstract</b> .....	<b>iii</b>
<b>Table of Content</b> .....	<b>v</b>
<b>1. Introduction</b> .....	<b>1</b>
<b>2. Objective and Research Question</b> .....	<b>4</b>
<b>3. Basics of Power Measurement</b> .....	<b>5</b>
<b>3.1 Electric Energy</b> .....	<b>5</b>
<b>3.2 Power in AC circuit</b> .....	<b>5</b>
<b>3.3 Sampling of Continuous-Time Signals</b> .....	<b>7</b>
<b>3.4 Power Measurement at the Institute of Production Engineering</b> .....	<b>9</b>
<b>4 Basics of Force Measurement</b> .....	<b>11</b>
<b>4.1 Turning</b> .....	<b>11</b>
<b>4.2 Milling</b> .....	<b>13</b>
<b>4.3 Force Measurement at the Institute of Production Engineering</b> .....	<b>16</b>
<b>4.3.1 Piezoelectric Technology in Dynamometers</b> .....	<b>16</b>
<b>4.3.2 Strain Gauge</b> .....	<b>18</b>
<b>4.3.3 Spike In-Process Measurement</b> .....	<b>19</b>
<b>4.3.5 Force Sampling Frequency</b> .....	<b>20</b>
<b>5 Basics of Ultrasonic Technology</b> .....	<b>21</b>
<b>5.1 Ultrasonic Vibrating Assisted Machining (UVAM)</b> .....	<b>21</b>
<b>5.2 DMG MORI Ultrasonic Machining</b> .....	<b>23</b>
<b>6 User Interface</b> .....	<b>24</b>
<b>6.1 Graphical User Interface (GUI)</b> .....	<b>24</b>
<b>6.2 Power and Force Analysis PAFA</b> .....	<b>25</b>
<b>6.2.1 Development</b> .....	<b>25</b>
<b>6.2.2 User Interface practice</b> .....	<b>29</b>
<b>6.2.4 Force and Energy</b> .....	<b>31</b>
<b>6.2.5 Energy Consumption Factor</b> .....	<b>33</b>
<b>6.2.6 Force vs Force</b> .....	<b>36</b>
<b>6.2.7 Energy vs Energy</b> .....	<b>38</b>
<b>6.2.8 Saving</b> .....	<b>39</b>
<b>6.2.9 Further development</b> .....	<b>39</b>
<b>7 Experiments and Results</b> .....	<b>40</b>

*Table of Content*

---

7.1	Power Measurement Settings.....	40
7.2	Specific Force $k_c$ determination .....	45
7.2.1	Conventional milling (Up-milling) .....	45
7.2.2	Climb (Down) milling.....	50
7.3	Tools and Machines .....	54
7.4	Test Methodology and Parameters .....	56
7.5	Force and Energy.....	58
7.7	Force vs Force .....	69
8	Conclusion and Further Outlook .....	70
	<b>List of Illustrations</b> .....	<b>72</b>
	<b>List of Tables</b> .....	<b>75</b>
	<b>Bibliography</b> .....	<b>76</b>
	<b>Appendix</b> .....	<b>79</b>

**List of Abbreviations**

<i>Abbreviation</i>	<i>Unit</i>	<i>Description</i>
$P$	W	Active Power
$U$	V	Voltage
$I$	A	Current
$p$	W	Instantaneous power
$\varphi$	-	Phase angle
$S$	VA	Apparent Power
$Q$	VAR	Reactive Power
$L1$	-	Phase 1
$L2$	-	Phase 2
$L3$	-	Phase 3
$E$	J	Energy consumption
$P_{ges}$	W	Total Active Power
$F_x$	N	Force in the X axis
$F_y$	N	Force in the Y axis
$F_z$	N	Force in the Z axis
$F_c$	N	Cutting Force
$a_p$	mm	Cutting depth
$a_e$	mm	Cutting width
$d_{drill}$	mm	Drilling diameter
$E_{processing}$	W.h	Energy demand of processing
$E_{spindel}$	W.h	Energy demand of Spindle
$f$	mm/rev	Feed rate
$f_z$	mm	Feed per tooth
$f_F$	kHz	Sampling rate Force
$f_V$	kHz	Sampling rate Voltage
$f_C$	kHz	Sampling rate Current
$n_w$	min <sup>-1</sup>	Workpiece rotational speed
$k_c$	N/mm <sup>2</sup>	Specific cutting force
$v_f$	m/min	Feed velocity
$v_c$	m/min	Cutting Velocity

*Table of Content*

---

$n$	1/min	Tool rotational speed
$z$	-	Number of teeth

PAFA: Power and Force Analysis

ECF: Energy Consumption Factor

ETS: Emission Trading Scheme

SME: Small and Medium Enterprises



## 1. Introduction

Reduction of CO<sub>2</sub> emissions and environmental footprint is a mandatory topic not only for industrialized countries but also for developing economies, many of them strongly dependent on non-renewable resources like coal, oil or natural gas as a basis for their energy utilization. Governments are then responsible for regulating the greenhouse gases by imposing protocols and setting strategies that help decreasing emissions. Within the European Union, for example, a regulatory framework called “Energy 2020” was first adopted in 2007 and set a target to reduce the greenhouse emissions by a minimum of 20% by the year 2020.<sup>1</sup>

In order to accomplish this goal, energy investments of around one trillion Euros will be needed. The most cost-effective manner to decrease emissions, expand energy security and make energy consumption cheaper for consumers is the modernization of equipment and infrastructure. These are central objectives of the 2020 policies that would improve energy efficiency.<sup>2</sup>

The industrial sector is one of the big players in the discussion as seen in Figure 1. Since 1990 to the present, it represents one of the three biggest energy consumption segments in Europe. However, although large companies are aware of this topic and have defined outlines such as the Emission Trading Scheme (ETS), small and medium enterprises (SMEs) are lacking energy management systems. A method to impulse the innovation and energy saving techniques is the efficiency benchmarking, a comparison method for power consumption that would measure the performance in terms of energy demand and grade the companies in relation to their competitors.

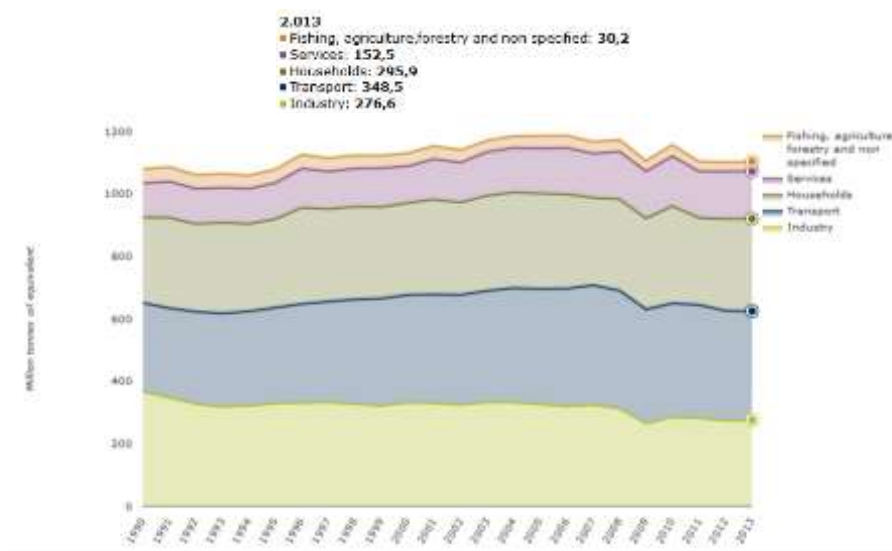


Figure 1. EU Final energy Consumption by Sector, Source: European Environment Agency, 2015

<sup>1</sup> Zein, 2012

<sup>2</sup> European Commission, 2016

More in detail, industry sector is the major consumer of electricity for over 20 years (see Figure 2). Since 2007, industry energy consumption is decreasing, mostly due to the economic crisis and it has been tough to show a real recovery. Expectations should indicate that some of the reduction is caused by the implementation of new technologies. In reality and stated by the European Association of Machine Tool Industries CECIMO, the age of the actual machinery park in some member countries with a strong manufacturing base has exceeded 19 years, when the average lifespan of a machine tool is 15 years.<sup>3</sup>

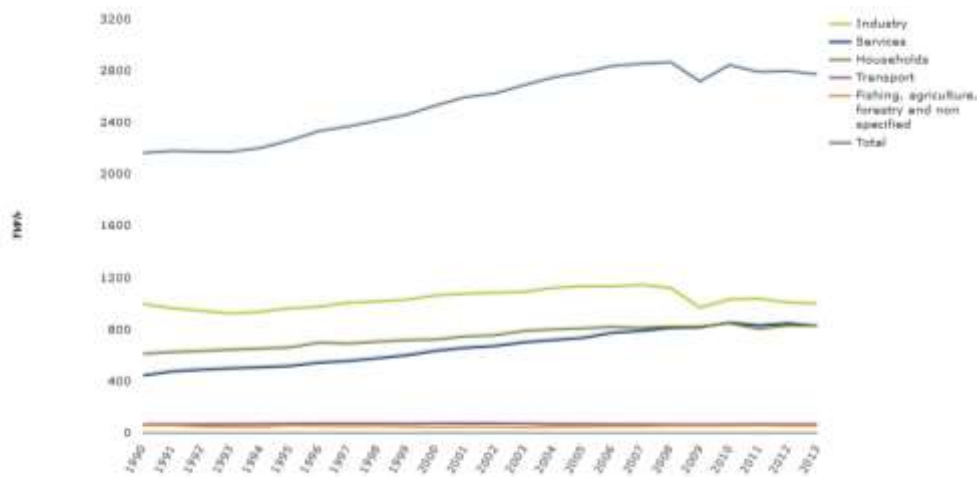


Figure 2. EU Final Energy Consumption of electricity by sector, Source European Environment Agency, 2015

Machining technology affects directly many different industrial sectors like aerospace, biomedical, and automotive because their manufacturing processes include parts that are shaped by removing material. Under machining, many different technologies are covered, such as cutting, grinding, thermal machining (Laser Beam Machining), plasma cutting and many others. Conventional machining processes like turning, milling and drilling are the bases of the machining industry and therefore the machines that carry on these practices and their improvement are fundamental for almost every industry.<sup>4</sup>

Although machines might be designed to reduce energy consumption while working a piece, small manufacturing companies do not often track the energy consumption due to the lack of an easy system that represents the energy consumption while an operating time. For companies with a wide range of products and therefore high time losses in tool changes and process setting, the stand-by consumed power should be as low as possible. On the other hand, machining equipment manufacturers make robust equipment in order to satisfy client needs, whenever his pieces require small or heavier cutting loads which tends to overestimate the real needs for a process.

<sup>3</sup> CECIMO, 2016

<sup>4</sup> Davim, 2011

In fact, industry researchers established that for modern CNC machining systems, the cutting energy only represents between 15% and 25% of the total consumed energy.<sup>5</sup>

Due to the complexity of the process and production devices, it is not simple to come with a solution for the energy waste reduction. However, instead of going into further and specific detail of the cutting process or mathematical models for all the different tools, standards to measure and analyze machining efficiency is needed. A simple way for a small/medium or big company, to recognize the appropriate and most effective machine for its own purpose. For this process, a standard test should be driven, data should be collected in standard formats and further evaluated. The results should then be available and with a significant and quantitative value. Machinery developers would then be focused on obtaining the lowest energy rates for the same procedures and developing better and low consuming systems, not only for the machining process itself but also for the standby operation state.

---

<sup>5</sup> Dahmus, et al., 2004

## **2. Objective and Research Question**

This project has as its main objective the design and development of an evaluation interface capable of executing an easy comparison between the force and power properties of a machining process.

Within the evaluation of those properties, it is important to be able to consider different machining tasks (turning, milling) and also to perform tests with different parameters like depth of cut, feed rate, rotational speed, material, machining tool size and many others.

Energy consumption, chip volume, and force loads are fundamental in the machines performance evaluation, therefore an objective of this project is also to be able to compare total machine capability considering a non-dimensional number developed at the Institute of Production Engineering.

As the spindle is the most important part of a mechanism during a machining process, the non-dimensional number will also be considered to compare spindle's performance between different machines.

Since ultrasonic technology is an innovative technology in the machining industry, where force loads are significantly reduced, the project will evaluate a simple material removal process and compare its performance with a traditional machining, following the same test parameters and intending to determine advantages and disadvantages of the utilization of the high frequency vibrations technology and its impact to influence energy consumption.

### 3. Basics of Power Measurement

#### 3.1 Electric Energy

Energy can be classified into four different groups: mechanical, thermal, electrical and electromagnetic radiation. In our case of study, we will be dealing with electrical energy as a representation of the flow of electrons, protons or ions. Energy consumption is derived from the electric power.

$$E = P\Delta t \quad [3-1]$$

Although the international unit for the energy is Joule, when evaluating energy consumption, is kWh (kilowatt hour) the most common derived unit.

Electric Power is established as the rate of electrical energy supplied to a circuit. Given a voltage  $U$  in an electric load and a flow of current  $I$  through the load, then is the Power  $P$  the multiplication of Current and Voltage. In direct current circuits DC, the current and voltage values remain constant over the time. For alternating current circuits, the voltage and current signals are fluctuating in every point of time. They have a periodical behavior.

#### 3.2 Power in AC circuit

An AC line in most of the cases provides a very clean voltage sine-wave. Depending on the load type, the current input might fluctuate and have a high distortion, normally harmonic signals. The instantaneous power is obtained by multiplying both instantaneous voltage and current.

$$p(t) = u(t).i(t) \quad [3-2]$$

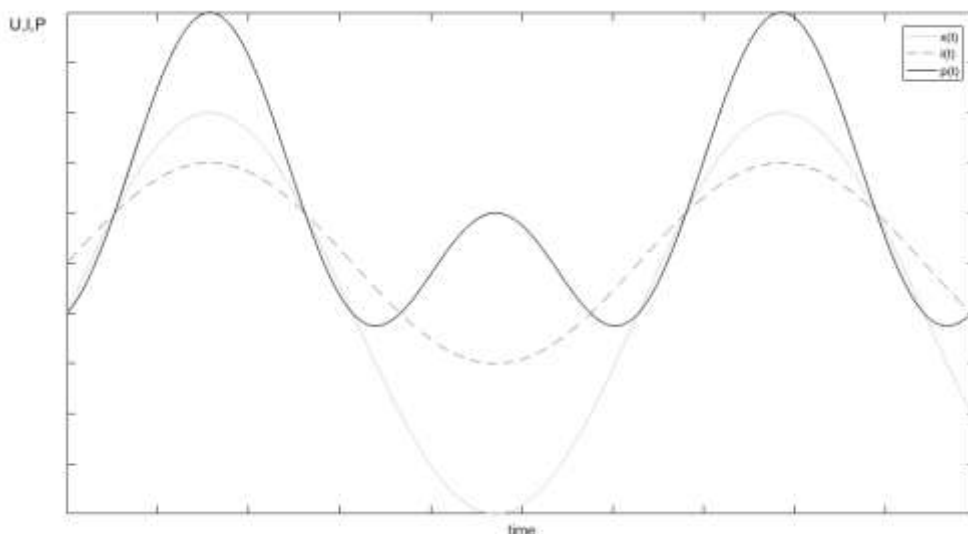


Figure 3. AC Signal example- Instantaneous Voltage, Current and Power, Source: Own contribution

The active power  $P$  is calculated as the mean value or the integral of the instantaneous power over a period of time.

$$P = \overline{p(t)} = \overline{u(t) \cdot i(t)} \quad [3-3]$$

$$P = \frac{1}{T} \int_T (u(t) \cdot i(t)) dt$$

The energy is then the area under the power curve (see Figure 4).

$$E = W = \int_{t=0}^{t=N} P(t) dt \quad [3-4]$$

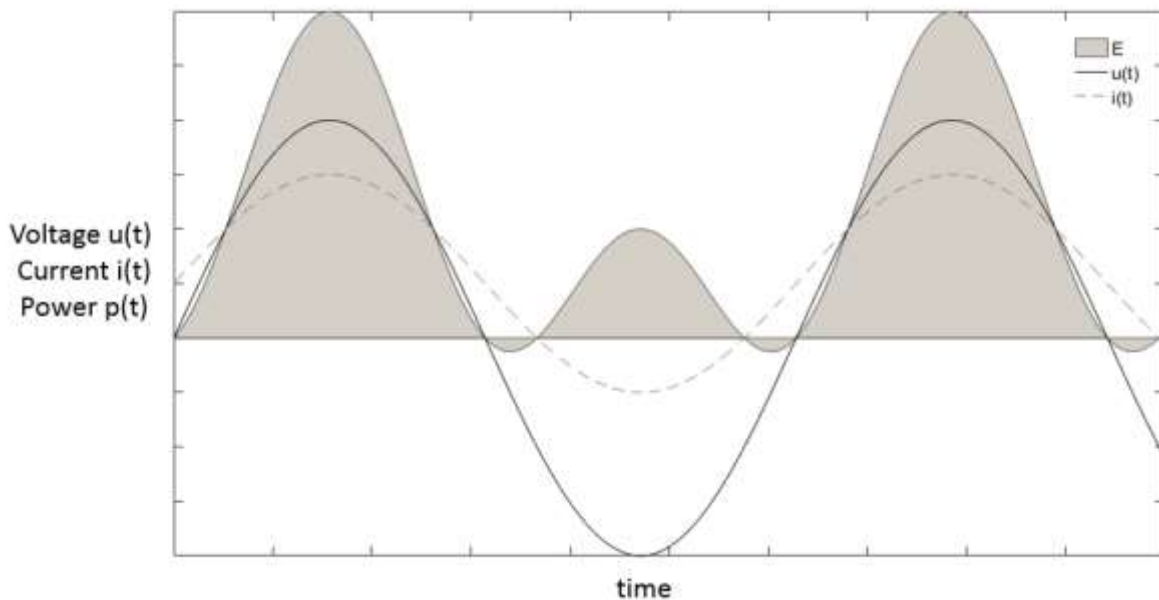


Figure 4. Active Power with phase shift, Source: Own contribution

In AC circuits the current and the voltage don't have the same phase. This phase shift  $\varphi$  is a result of capacitive or inductive loads that can store energy, called reactive power  $Q$ .

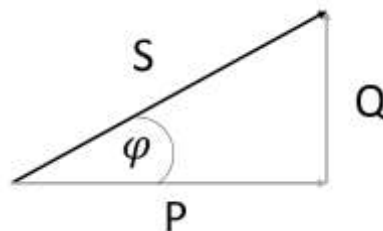


Figure 5. Vector Representation  $P$ ,  $Q$ ,  $S$ , and  $\varphi$ , Source: Own contribution

Where  $S$  is the apparent power. For the case of study, the negative power areas under the curve are minimal and therefore is not necessary a further calculation of the active power but simply calculating the multiplication of instantaneous current and voltage.

For a three phase system the instantaneous power is still calculated as the product between current and voltage of each phase and. There will be 3 power lines and the total power is the sum of them. The energy consumption is the integral of the total power during over certain period of time.

### 3.3 Sampling of Continuous-Time Signals

Voltage and current are continuous signals which can be represented in a discrete form through periodic sampling. These samples sequence  $x[n]$  are related to the continuous signal in the following form:

$$\mathbf{x[n] = x_c(nT), \quad -\infty < n < \infty} \quad \mathbf{[3-5]}$$

$T$  is the sampling period and the sampling frequency in samples per second will be its reciprocal  $f_s = 1/T$ . When measuring physical phenomena, the sampling is implemented by an analog to digital (A/D) converter that approximates the ideal continuous to digital (C/D) converter. However, this approximation is strongly dependent on parameters like quantization of the output sample, linearity of the quantization, sample and hold circuits and sampling rate limitations.<sup>6</sup>

#### Frequency Domain Representation

This is a tool of high relevance in signal processing applications. In comparison to a time domain analysis which represents the changes of a signal over the time, frequency domain analysis shows the energy distribution of a signal over a range of frequencies. It also includes information about the phase shift that has to be applied to each frequency component to compose the original time signal as a combination of the single frequency elements.

A transform is a mathematical operator that can convert the time and frequency domains. One of the most common transforms in the engineering field is the Fourier transform which decomposes a function into the sum of multiple sine wave frequency elements. The frequency domain representation of the signal is called spectrum.

Periodic signals like the voltage and current in this case of study, are simple to observe with oscilloscopes and Fourier transform that allows an easier characterization of systems in an algebraic form compared to differential equations in the time domain representation.

---

<sup>6</sup> Oppenheim, et al., 2010 pp. 153-155

The spectrum of a signal  $x(t)$  gives a hint of the multiple important frequencies. The so called fundamental frequency, is the lowest frequency of a periodic waveform. Figure 7 shows a time periodical signal composed of multiple sine waves is shown and also its frequency domain representation.

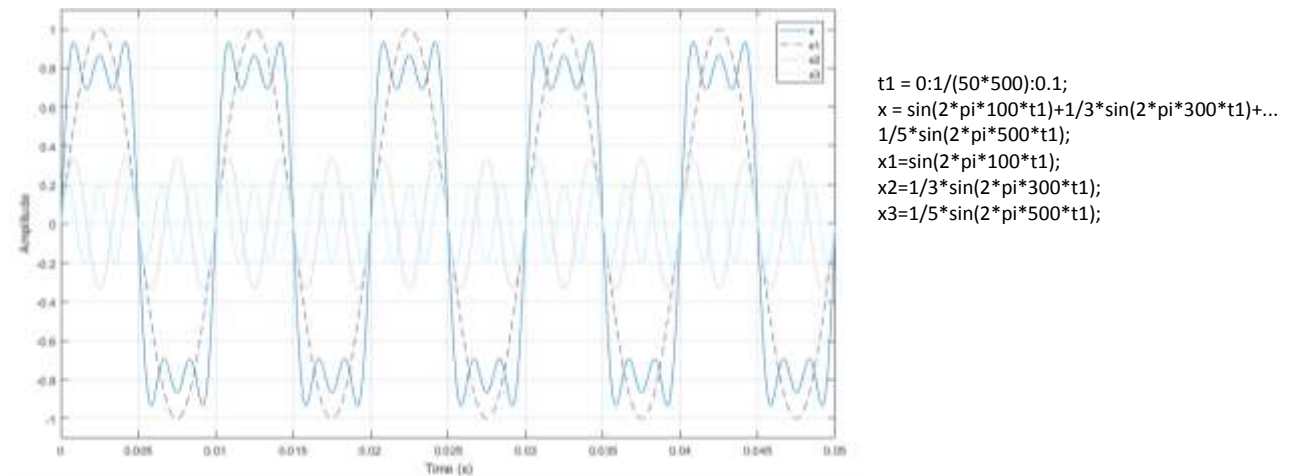


Figure 6. Periodical Signal Time Domain Representation, Source: Own contribution

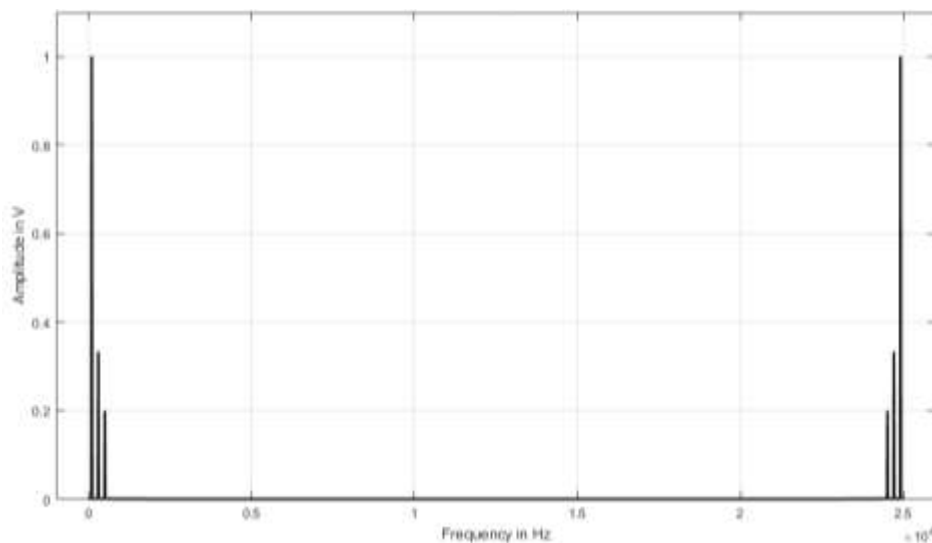


Figure 7. Periodical Signal Frequency domain Representation, Source: Own contribution

The fundamental frequency is 100 Hz and the highest frequency is 500 Hz, both of them within the bandwidth range. Following the Nyquist-Shannon Sampling Theorem, the sampling rate needed for capturing all the information from a continuous time signal has to be bigger than twice the highest frequency of the signal, in this case at least 1000Hz. However, this theoretical approach does not always match practical implementations.<sup>7</sup>

<sup>7</sup> Oppenheim, et al., 2010 p. 553



### 3.4 Power Measurement at the Institute of Production Engineering

The DEWETRON Data Acquisition system is used to execute the power measurements. It is a portable device consisting as shown in Figure 8 of the main unit (DEWE 30-16) that includes twelve modules, each one can be used then to measure voltage or current.

The acquisition system consists also of three current amplifying clamps (Dewetron PNA-CLAMP-150-DC) with their corresponding power box, three current amplifying coils (Dewetron PNA-A100-300-45), and the correspondent voltage cables with banana plugs. Technical data of the devices can be found in Table 1.

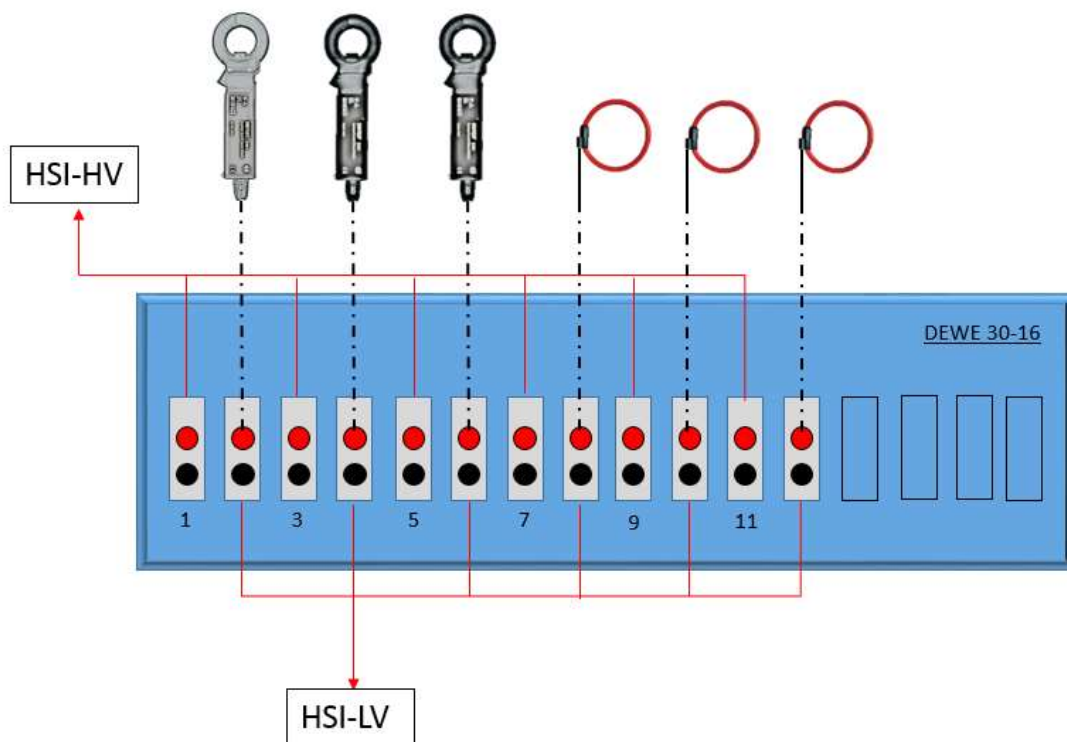


Figure 8. Power Measurement System, Source: Own contribution

The current measurement devices convert the current input signal into a voltage signal and send it to the low voltage modules HIS-LV [ports 2,4,6,8,10,12]. The voltage signals are connected to the high voltage amplifiers HIS-HV [ports 1,3,5,7,9,11].

The data is sent from the main unit *DEWE 30-16* modules through the analog/digital “DE-C03xx” cable to the DEWE-ORION-16-16 board previously installed in the PC. The modules send the signals as an analog input in a range of  $\pm 5V$ .<sup>8</sup>

<sup>8</sup> DEWETRON Elektronische Messgeraete Ges. m.n.H., 2012

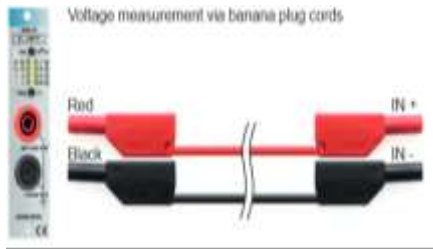




Device	HIS-LV-B module	HIS-HV module	DEWE-ORION-16-16
View			
Main Features	<p>Range: 12 ranges (10 mV to 50 V)</p> <p>Accuracy: <math>\pm 1\%</math> Range</p> <p>Output Voltage: <math>\pm 5</math> V</p> <p>Max. Frequency: 2 MHz</p>	<p>Range: min <math>\pm 20</math> V max <math>\pm 1400</math> V</p> <p>Accuracy: <math>\pm 1\%</math> Range</p> <p>Output Voltage: <math>\pm 5</math> V</p> <p>Max. Frequency: 2 MHz</p>	<p>Max Freq: 100kSamples/sec per channel</p> <p>Inputs: 16 analog</p> <p>Input Ranges: 4 from</p>
Device	DEWE 30-16	PNA-CLAMP-150-DC	PNA-A-100-300-45
View			
Main Features	<p>Sockets: 16</p> <p>Output signal: 68-pin SUB-D</p>	<p>Range: 12 ranges (10 mV to 50 V)</p> <p>Accuracy: <math>\pm 1\%</math> Range</p> <p>Output Voltage: <math>\pm 5</math> V</p> <p>Max. Frequency: 2MHz</p>	<p>Range: min <math>\pm 20</math>V max <math>\pm 1400</math>V</p> <p>Accuracy: <math>\pm 1\%</math> Range</p> <p>Output Voltage: <math>\pm 5</math>V</p> <p>Max. Frequency: 2 MHz</p>

Table 1. Technical Data Dewetron Acquisition System, Source: DEWETRON Elektronische Messgeraete Ges. m.n.H., 2012

## 4 Basics of Force Measurement

Force measurement in the production is a basic indicator to control the interaction between workpiece and tool. Important further factors such as tool wear and surface finish are used to compare processes and improve the machinability. According to the type of machining, the main parameters and therefore the force calculations change. Some of the most common industrial processes will be described with their main process parameters.

### 4.1 Turning

Turning is defined as a group of machining operations where the workpiece is permanently rotating as the tool executes the feed motion. In the Figure 9, different basic turning motions are shown, according to the feed motion direction.

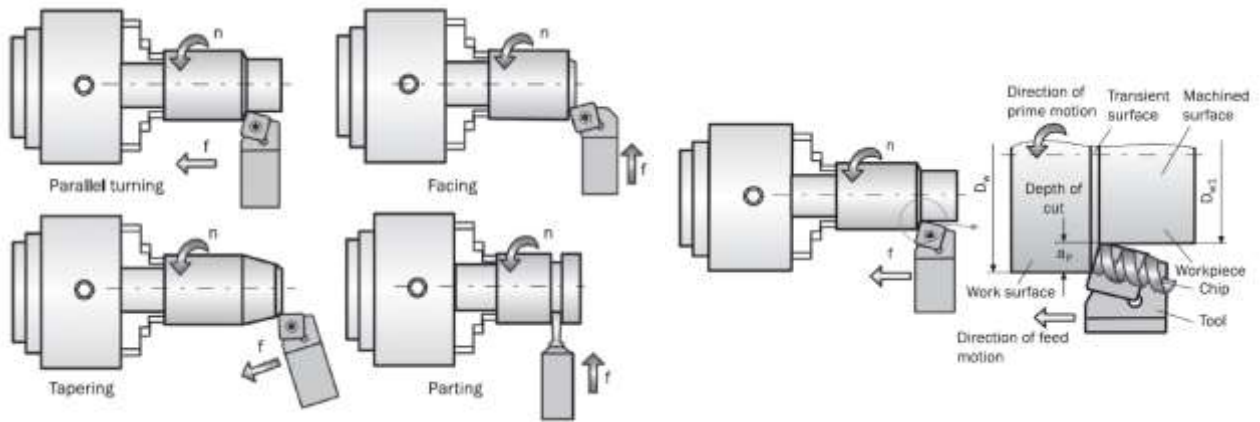


Figure 9. Left: Basic motions in turning operations, Right: Components of the machining, Source: Astakhov, 2011

$$\text{Cutting Speed: } v = \pi D_w n \text{ in m/min} \quad [4-1]$$

Where  $n$ : rotational speed ( $\text{min}^{-1}$ ) and  $D_w$ : workpiece diameter (m)

$$\text{Cutting Feed: } f \text{ in mm/rev} \quad [4-2]$$

$$\text{Feed rate } v_f = f \cdot n \text{ in mm/min} \quad [4-3]$$

$$\text{Depth of cut : } a_p = \frac{D_w - D_{w1}}{2} \text{ in mm} \quad [4-4]$$

$$\text{Material Removal Rate : } MRR = f \cdot v \cdot a_p \text{ in } mm^3/min \quad [4-5]$$

### Cutting Forces

The resultant force  $R$  is a 3D vector (see Figure 10). It is important to keep a consistent coordinate system while machining a piece since the measurement systems use the Standard ISO reference coordinates. The main movement is marked with the y-axis and the z-axis follows the feed motion direction.

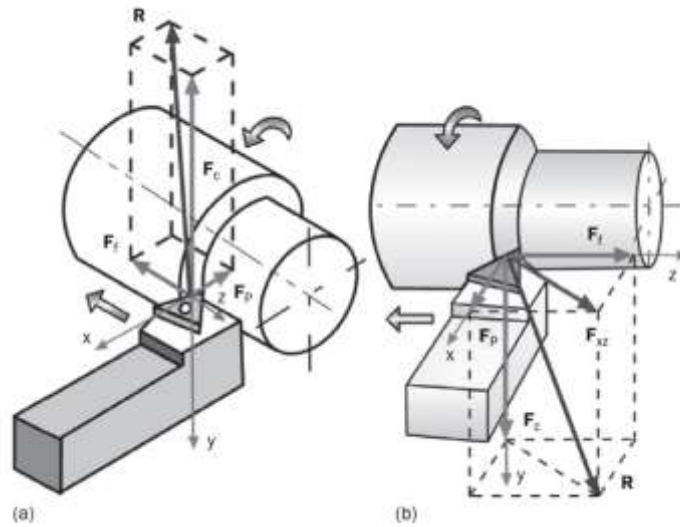


Figure 10. Cutting Force Components, Source: Astakhov, 2011

The tangential force  $F_c$  is the main value for power calculation. There are also the axial force  $F_f$  and the radial force  $F_p$ .

### Cutting Power

Power is defined as the multiplication of the resultant force and the velocity in its direction. The different force and velocity components are multiplied, however in the turning process the radial force  $F_p$  is zero, and the axial Force  $F_f$  is very small when compared to the tangential force and therefore it can be ignored. The cutting power is finally the product of the tangential force and the cutting speed.

$$P_c = F_c \cdot v_c \text{ in } W \quad [4-6]$$

The specific cutting power  $P_{c-c}$  is the above-shown value divided by the volume of material removed.

$$P_{c-c} = \frac{F_c v_c}{MRR} = \frac{F_c}{f a_p} \text{ in } W/mm^3 \quad [4-7]$$

## 4.2 Milling

It is the most commonly used machining operation basically due to its versatility. The cutting tool has multiple edges and does both a rotating movement and a feed movement that can be done in multiple directions according to the desired final shape. Each time one of the edges contacts with the workpiece, a small amount of material is removed and therefore a chip that is easy to take away.

A milling tool has several cutting edges and each of them has two cutting faces: the major and the minor edge. The first one is tangential to the tool body and removes the material; the minor is facing perpendicular to the tool axis and is in charge of the final surface roughness.<sup>9</sup>

The angle between the workpiece and the major edge is called position angle  $K_r$ , and it affects the cutting force components  $F_x$  and  $F_y$ , the chip thickness and the tool life.

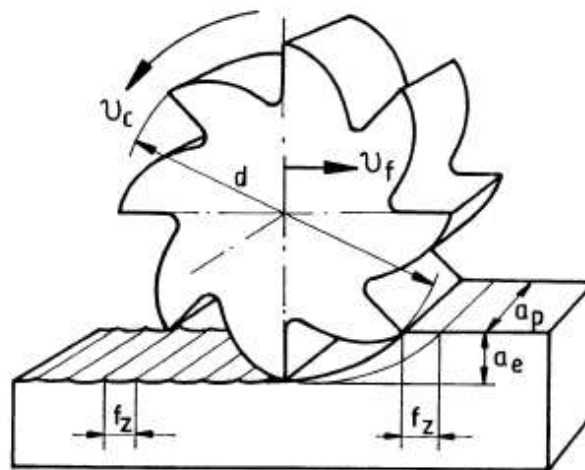


Figure 11. Force Contact conditions, Source: Eberhard, et al., 2008 p. 215

Main parameters:

**Cutting Speed  $v_c$ :** Tangential peripheral velocity on the cutting edges

$$v_c = \pi \cdot n \cdot d \text{ in m/min} \quad [4-8]$$

Where  $n$ : rotational speed ( $\text{min}^{-1}$ ) and  $d$ : tool diameter (m)

Feed per tooth  $f_z$ : Distance traveled by the tool in a single rotation divided by the number of teeth.

<sup>9</sup> Lacalle, 2011

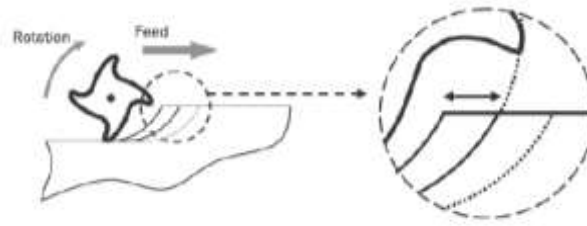


Figure 12. Feed per tooth for milling, Source: Lacalle, 2011

$$v_f = f_z \cdot z \cdot n, \text{ in m/min} \quad [4-9]$$

Where  $v_f$  is the feed rate,  $z$ : number of teeth and  $n$ : rotational speed

Engagement: Axial depth of cut  $a_p$ (mm) and Radial depth of cut  $a_e$ (mm)

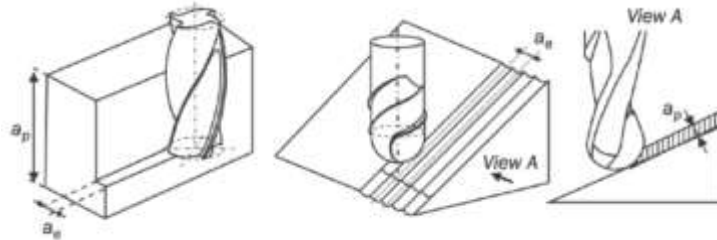


Figure 13. Axial and radial depths of cut, Source: Lacalle, 2011

Material Removal Rate (MRR):

$$MRR = v_c A_c = v_c h b, \text{ in mm}^3/\text{min} \quad [4-10]$$

$A_c$  is the chip section,  $h$  the chip thickness, and  $b$ , the chip width. For some cases (Figure 13 left) is  $h = a_e$  and  $b = a_p$ .

### Force and Power in Milling

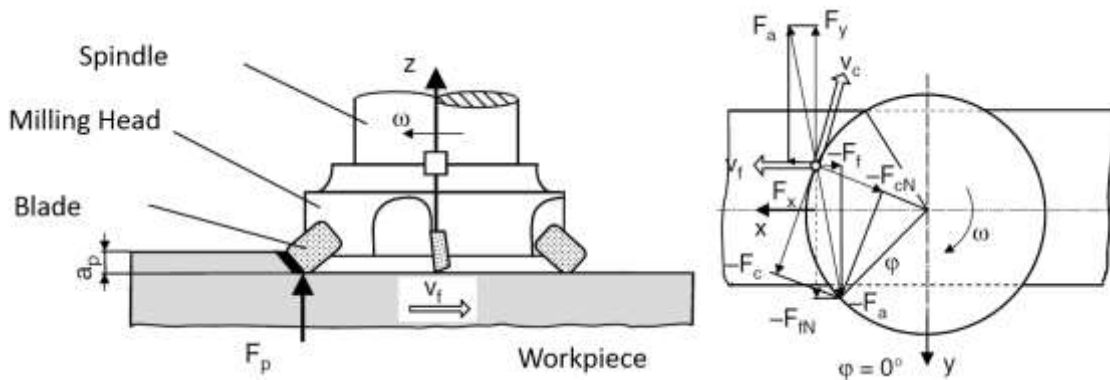


Figure 14. Left: Milling Process and main Parameters, Right: Forces Description, Source: Berend, et al., 2011

Force components  $F_c$  and  $F_{cN}$  can be calculated through a transformation of the Cartesian coordinate forces.

$$\begin{bmatrix} F_c \\ F_{cN} \\ F_p \end{bmatrix} = \begin{bmatrix} \sin \varphi & -\cos \varphi & 0 \\ \cos \varphi & \sin \varphi & 0 \\ 0 & 0 & 1 \end{bmatrix} * \begin{bmatrix} F_x \\ F_y \\ F_z \end{bmatrix} \quad [4-11]$$

This approach is used for practical force measurements (piezoelectric system). The cutting power is the product between the cutting force and the cutting velocity.

$$P_c = F_c \cdot v_c, \text{ in } W \quad [4-12]$$

### 4.3 Force Measurement at the Institute of Production Engineering

There are two main types of dynamometers for machining applications. The stationary is set on the table of the machine tool and the rotating dynamometers mounted directly on the machine spindle.

#### 4.3.1 Piezoelectric Technology in Dynamometers

The main characteristics of this system are the high linearity that the sensors provide and the rigid construction of the device and the piezoelectric crystals. The main advantages of this technology are the large measurement range although large dynamometers are used, and the high natural frequencies that can be achieved.<sup>10</sup>

The main principle behind the piezoelectric dynamometers is the material of the sensors as their name indicates. Piezoelectric sensors generate a proportional charge to the effective load. The sensors are sensitive in only one direction and are cut out of crystal bars according to the measurement direction. In Figure 15 left, a stationary 3-component Dynamometer is shown, containing four sensors that allow the measurement of the components ( $F_x, F_y, F_z, M_x, M_y, M_z$ ). The torques are calculated from the force components.

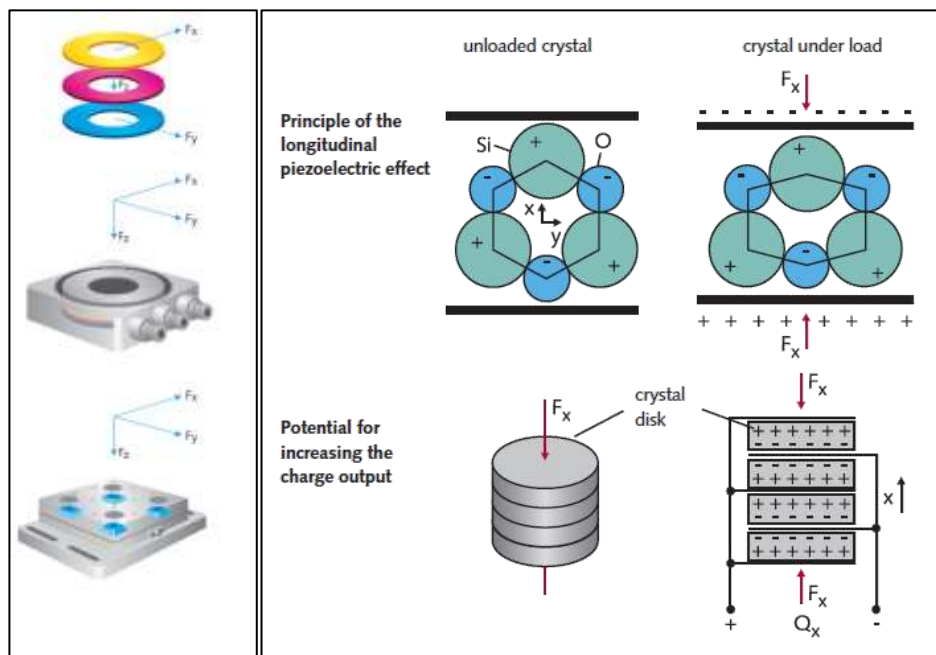


Figure 15. Piezoelectric Dynamometers. Left: Stationary 3-Component Dynamometer, Right: Longitudinal effect, Source: KISTLER Group, 2014

<sup>10</sup> KISTLER Group, 2014



There are two effects distinguished during the measurement, the longitudinal and the shear effect. As shown in the Figure 15 right, when a crystal is exposed to vertical loads, small changes in the center of gravity of the charge occur in the disk. The same applied for the shear effect and the charge differences are carried to the amplifier, then converted into voltage signals (see Figure 16).

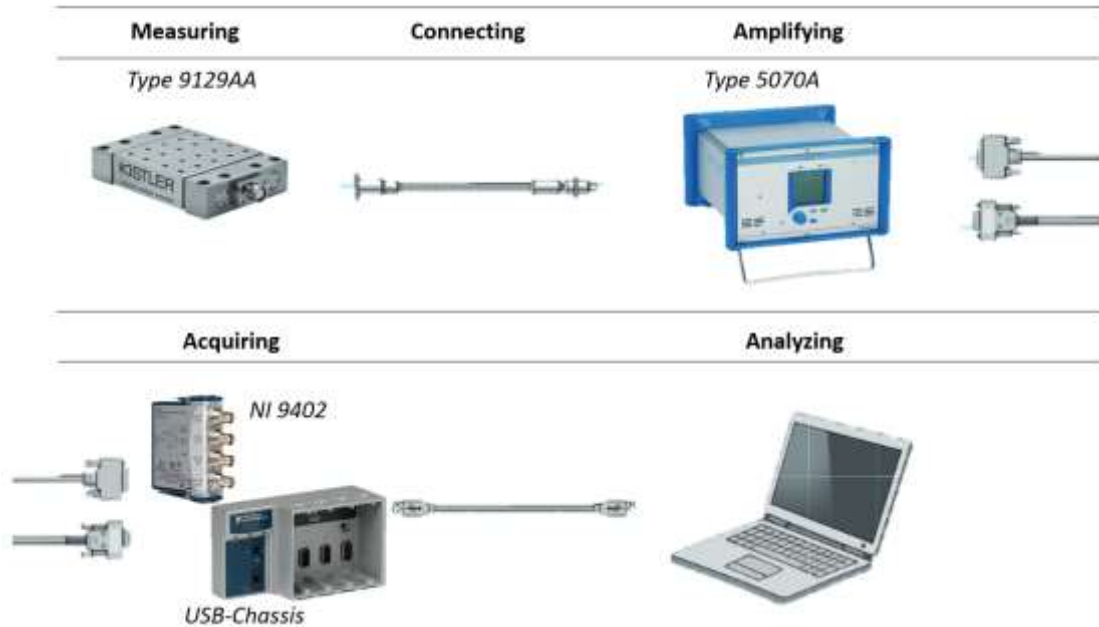


Figure 16. Measuring Chain for stationary Dynamometer, Source: KISTLER Group, 2014

Equipment	Reference
Measurement Platform	KISTLER 9129AA Multicomponent Dynamometer
Amplifier	KISTLER 5070A Multi-Channel Charge Amplifier
Chassis for Data Acquisition	NATIONAL INSTRUMENTS USB-Chassis
Data Acquisition Module	NATIONAL INSTRUMENTS 9402 Digital Input-Output

Table 2. Measurement Chain Equipment Reference (KISTLER + National Instruments)

### 4.3.2 Strain Gauge

One of the simplest but most effective methods to measure strain, to afterwards determine the applied force, is the application of a strain gauge on a workpiece. Due to the type of material which the gauge is made of, the resistance of the gauge changes linearly in proportion to the amount of strain. The most commonly used gauge is the bonded metallic strain gauge that consists of a foil arranged in a grid pattern in the parallel direction to the displacement (see Figure 17). The grid is attached to a support called barrier and is directly attached to the test specimen. <sup>11</sup>

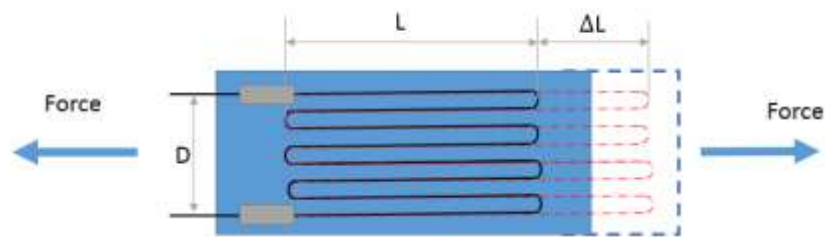


Figure 17. Strain Gauge before and after axial force is applied, Source: Own contribution

Depending on the type of load applied (axial or bending), strain gauges vary. Quarter Bridge, half bridge and full bridge (see Figure 18). Also, depending on the desired accuracy of the measurements, the selection of the gauges differ. Some of these selection parameters are length, price, tolerances, reliability, etc.

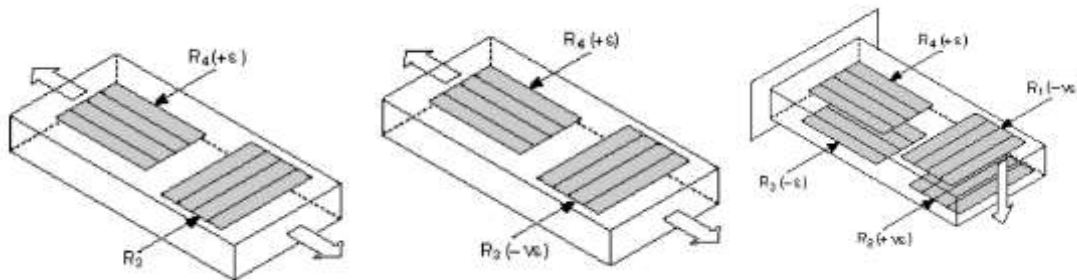


Figure 18. Examples of Gages Types: Left: Quarter-Bridge, Center: Middle Bridge, Right: Full Bridge, Source: National Instruments, 2016

<sup>11</sup> National Instruments, 2016

### 4.3.3 Spike In-Process Measurement

Promicron, a German company for wireless measurement systems and sensors, developed a tool holder like shown in Figure 19. It is able to measure the forces and torques during the machining process (drilling, milling, grinding, tapping, etc.). The system measures real-time data and sends it wireless to a receiver that is connected to a data processor<sup>12</sup>.

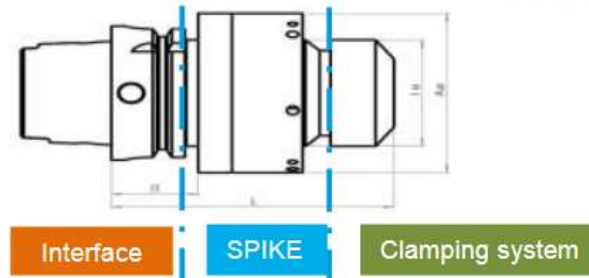


Figure 19. Spike integration into a machining system, Source: Promicron, 2016

The most important feature of this system is the operability due to the non-cables solution. The system can measure 4 channels which include: Axial force, Torque, X-Axis bending and Y-Axis bending. More technical data of the system can be found in Table 3.

Automatic tool changer compatibility	Yes
Number of wireless channels	4
Data transmission frequency	2,45 GHz
Sampling rate per channel	Max. 1,6 kHz
Resolution of measured values	15 bit
Maximum allowed rotational speed	18.000 rpm
Signal transmission range	2-3 m
Battery life	8 hours
Charging time	4 hours
Coolant system compatibility	Inside/Outside
Raw data Output	.txt file

Table 3. Technical Data SPIKE measurement system.<sup>13</sup>

<sup>12</sup> Promicron, 2016

<sup>13</sup> Promicron, 2016

### 4.3.5 Force Sampling Frequency

According to the rotational speed of the machining process, enough information should be collected in order to construct a discrete signal representing every single angle (from 0° to 360°) the cutting plate goes through during the process.

With a given rotational speed  $n$  ( $min^{-1}$ ), the minimum sampling frequency is then defined as:

$$f_{min} = \frac{n \cdot 360^\circ}{60} = n \cdot 6, \text{ in Hz} \quad [4-13]$$

## 5 Basics of Ultrasonic Technology

A big topic for the machining industry is to consider the impact on the environment. When talking about machining of some specific materials, most of the metals or alloys, it is very common to relate the use of fluids and lubricants during the cutting process. The usage of these fluids requires a high amount of resources and therefore an adequate disposal of them and the rise of the manufacturing costs. In that matter, reduction of removal of these resources and therefore expenses can be achieved through a proper dry machining many times not feasible for high accuracy applications.<sup>14</sup>

Ultrasonic assisted machining (UAM) has become then the right technology for improving the machining process, not only because of the elimination of fluids during the machining, but also because of the advantages of the finished working piece.

### 5.1 Ultrasonic Vibrating Assisted Machining (UVAM)

Ultrasonic vibrating assisted machining is a combinatory technique consisting in the application of an ultrasonic vibration at a frequency above the audible range (over 20000 Hz) with the movement of a cutting tool. The amplitude of the vibration movement is small, usually not over 20 microns. It has been demonstrated that the simple traditional machining techniques can be improved in a high manner. It is commonly used for small details in hard material like glass, ceramics, composites and precious stones. Many of these materials are characterized by low ductility and a hardness above 40 HRC.<sup>15</sup>

When all the process parameters (cutting velocity, tool amplitude and frequency) are selected properly, thinner chips are generated due to the periodical constant loss of the tool with the chip (see Figure 20) and therefore lower cutting forces are present. Depending on the material, this reduction can go up to 80% (aerospace super alloys). On this case, cutting velocity is done in the X-axis and the vibration in the Z axis.

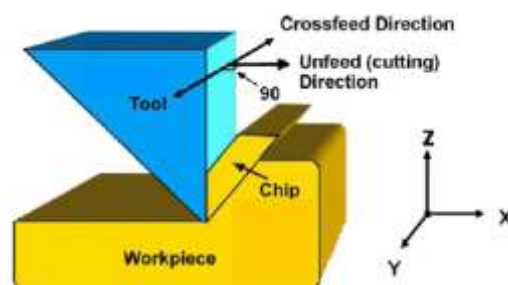


Figure 20. 1 Dimension Vibration Assisted Machining, Source: Review of vibration-assisted machining, 2007

<sup>14</sup> Maurotto, et al., 2015 p. p1

<sup>15</sup> Silberschmidt, et al., 2014

In comparison to other non-traditional techniques like laser beam and electrical discharge machining, the ultrasonic machining does not produce thermal damage to the workpiece or significant residual stresses. Vibration Assisted Machining has been developed enough to be included in many industries. However, there is still some theoretical development missing.<sup>16</sup> There are three types of Vibrating Assisted Machining: 1-Dimensional, 2-Dimensional Resonant and 2-Dimensional Non-Resonant VAM system. Figure 21 shows the difference of the instantaneous forces between a linear and a conventional process.

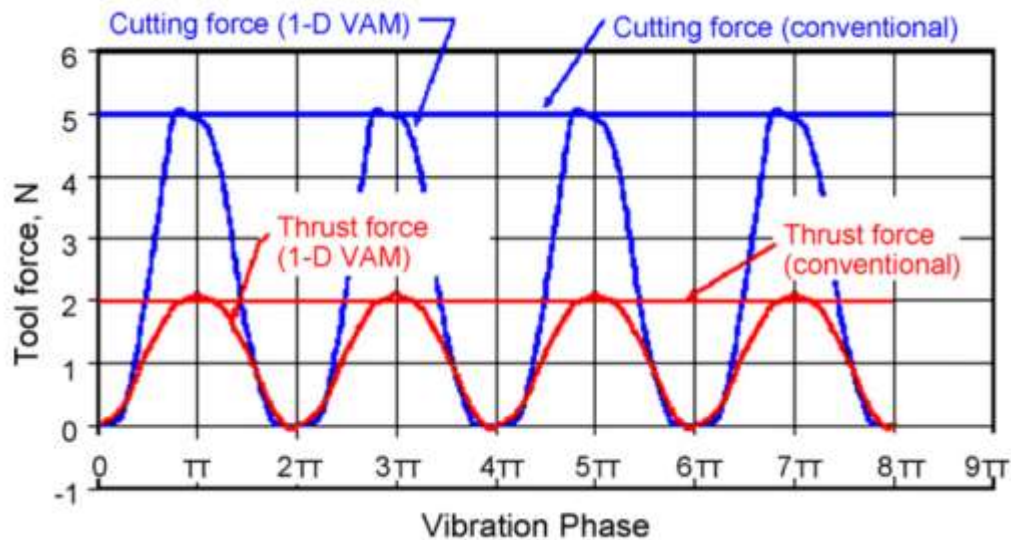


Figure 21. Tool force comparison between linear VAM and conventional cutting, Source: Review of vibration-assisted machining, 2007

The following chart developed by researchers at the Loughborough University shows clearly the force reduction within a turning practice. This process was developed with the possibility to switch on and off the vertical ultrasonic vibration during the machining, in order to provide the possibility of comparison.

Two important factors to be considered for this project are the material removal rate and the power consumption due to the ultrasonic generator. Power ratings vary typically from 50 to 3000 W and can even reach 4kW in some machines.<sup>17</sup> The material removal rate MRR is dependent on the amplitude of the movement in the Z axis. MRR generally increases proportionally with the amplitude.<sup>18</sup>

<sup>16</sup> Brehl, et al., 2007

<sup>17</sup> THOE, et al., 1997 p. 239

<sup>18</sup> THOE, et al., 1997 pp. 245-247

## 5.2 DMG MORI Ultrasonic Machining

DMG MORI Seiki is a Japanese-German Company that manufactures machine tools. Their most important products are of CNC lathes, milling machines, turning centers, horizontal machining centers, five-axis turning centers, and many others. The Institute of Production Engineering has one of the latest machine tools available for pieces manufacturing and studies, the ULTRASONIC 30 linear. It is a 5 axis simultaneous machine tool that can be used for conventional machining processes and for precision machining of advanced materials. Some of the multiple applications can be seen in Figure 22.

Its main characteristics include the dynamic drives (up to 50 m/min traverse speed). It also has a swivel range in the B axis of  $\pm 120^\circ$ . The spindle can reach up to 40.000 rpm and a 30 fold tool magazine. Another interesting aspect is the operational system CELOS, a holistic user interface that makes the machine operation intuitive and easy. This system accelerates operation set-up.<sup>19</sup>



Figure 22. Machining Strategies for ULTRASONIC 30 linear, Source: DMG MORI, 2016

Examples of DMG MORI ULTRASONIC Industry applications:

- Aerospace: Housing structures, blades, armatures
- Optics: Lenses, spheres, glass.
- Watch: Fine mechanical parts (housing, plates)
- Dental: Dentures, Implants, Prosthetics

<sup>19</sup> DMG MORI, 2016

## 6 User Interface

### 6.1 Graphical User Interface (GUI)

GUI is a designed digital space that allows the interaction between a user (human) and a software or hardware (or both), through visual representations. According to the input provided by the user, the device executes specific operations and gives an output which will be then seen by the operator, responsible for either controlling a system or evaluating a process.

The main goal of such an interface is to improve the productivity of a system, reducing to the highest point the complexity and leaving simple commands for the user to access to run a process, evaluate, or control it. There are several software and languages available to program and design a user interface, for example in the engineering field some of the most common are C++, Python, Labview, or MATLAB. MATLAB is the one implemented for the actual analysis just like the previous force data acquisition software developed at the Production Engineering Institute. This way a complete consistent measurement and comparison for system are established.



## 6.2 Power and Force Analysis PAFA

### 6.2.1 Development

#### Offline Data Analysis and time difference of the measurements

It is important to mention that the PAFA software is intended to work offline, this means, that the data has to be previously measured. The power acquisition with the Dewetron system cannot be linked to MATLAB instantaneously but has to be acquired with the DEWESOFT software and afterward exported into a MATLAB file.

Since the User Interface should show a plot with both force and power data, the time variable represented a big challenge during the software development because the starting point of the measurements was not the equal, due to the software difference. First, the power measurement (DEWESOFT) was set to store the data and after the force measurement (NI-DAQ).

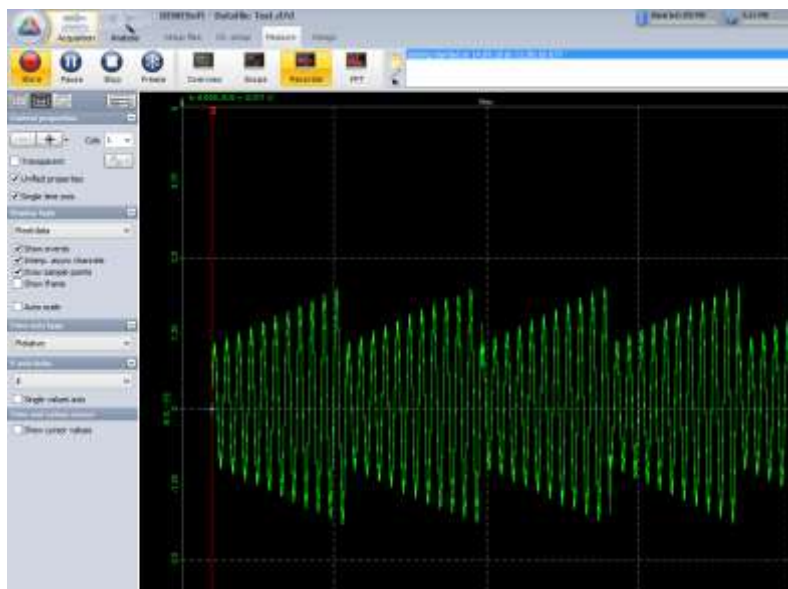


Figure 23. Dewesoft Recorder, Source: Own contribution

The time vector of one of the software had to be modified to correct the difference between the storage starting points. The initial ideas are related recognizing in both measurements the start of the machining (since both power and force increase significantly) and build a time vector based on that point. This solution works for processes where the force differences are clear enough. Unfortunately, for some force tests where depth of cut is lower than 1 mm, the components do not change clear enough to establish a starting point of the machining.

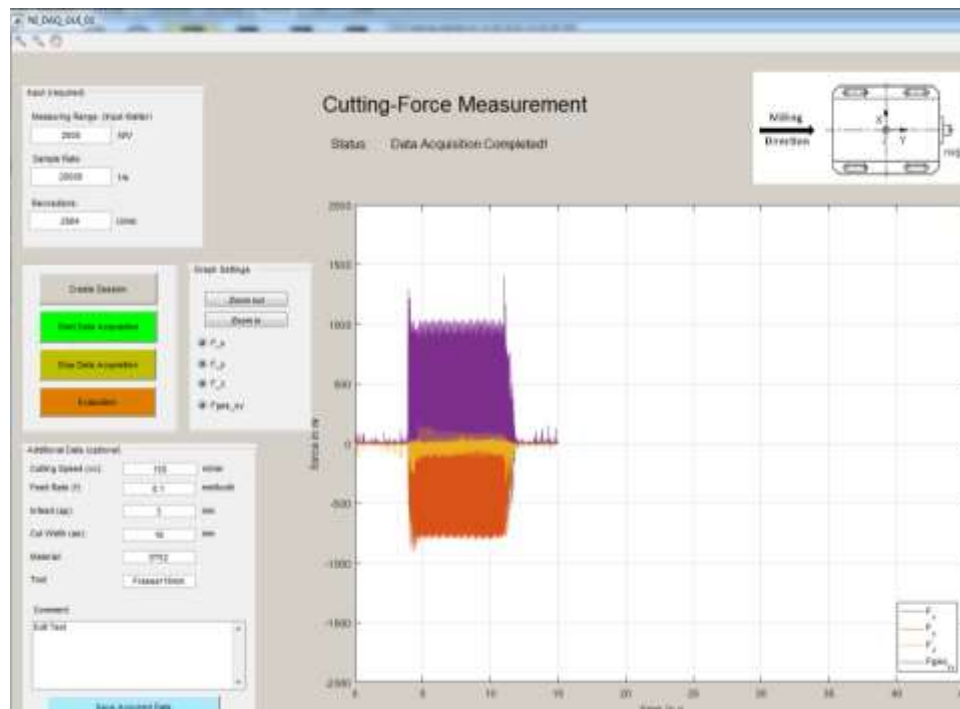


Figure 24. Cutting Force Data Acquisition, Source: Own contribution

A better solution has to be found and it should be noticed that the Dewesoft Software automatically creates a *Start\_Time* figure when the storage starts and saves it into the measurement file. With that in mind, the Force Data Acquisition was slightly modified and a *Force\_Starting\_Time* figure was created, based on the Matlab function “clock” that returns a six element date vector containing the current time and date in decimal form.<sup>20</sup>

### Initial Force Data Evaluation Interface

The BOF user interface for force data evaluation was developed by Ewald Grabner from the Production Engineering Institute and it allows the upload of the Force data and then chooses a specific area of cutting where only one or a few revolutions are shown (see Figure 25). Afterward, an initial point is chosen by the user to identify where one of the blades starts with its contact to the working piece. Through the equation matrix [4-11] both cutting force and radial force are calculated and shown in a second plot where the x-axis does not represent the time but the angular position.

<sup>20</sup> Grabner, 2016

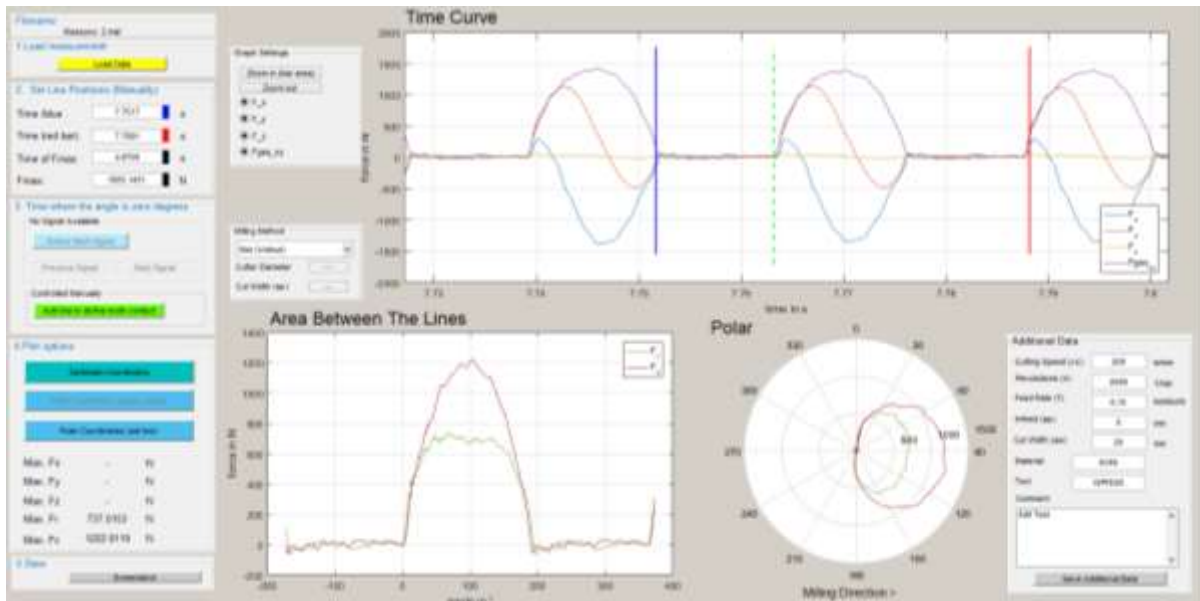


Figure 25. User Interface for the Force Data Evaluation, Source: Grabner, 2016

The cutting force and radial force calculation are important for the posterior Energy Consumption Factor.

### Power Data Extraction and Upload into MATLAB

Power data, specifically current, voltage, and time vectors are stored by the DEWESOFT software and after exporting the full speed data into a MATLAB file, they could be loaded by the BOF software. Variables were identified in MATLAB according to the way they are named in DEWESOFT. For example when measuring the first channel was called Spindle\_Voltage\_L1 and the second Spindle\_Current\_L1. After exporting the data the names would include "Data1\_" before the initial names. A MATLAB code was developed to identify first the element name, then the variables name and finally the measured phase. However, after evaluating the software several times it was realized that identifying variables according to the name is not the best alternative since the possibility of a mistype during the measurement is high.

A more simple and effective recognition method is developed, that would consider the order of the measured channels. When having 12 measurement channels available, the first 6 would be then used for one element (Spindle, Lubricant, Total Machine or any other) and the second 6 channels for another element. The code would automatically recognize if only one of two elements were measured and assign the data arrays to a current or voltage variable.

To avoid mistakes in the polarity of the current measurements, a correction factor was also implemented, which calculates the power and if the mean value was negative, it meant that the current was measured with inversed polarity. The correction was simply multiplying the current vector by -1.

Power Data Evaluation

There is an initial modification to the force interface (BOF), adding a fourth plot for the power data. However, this implementation makes the interface more complex to understand (see Figure 26) which goes in the wrong direction with the project objectives. The design of a completely new user interface is implemented, where just smart and important data are shown and only a simple chart would include both, force and power data.

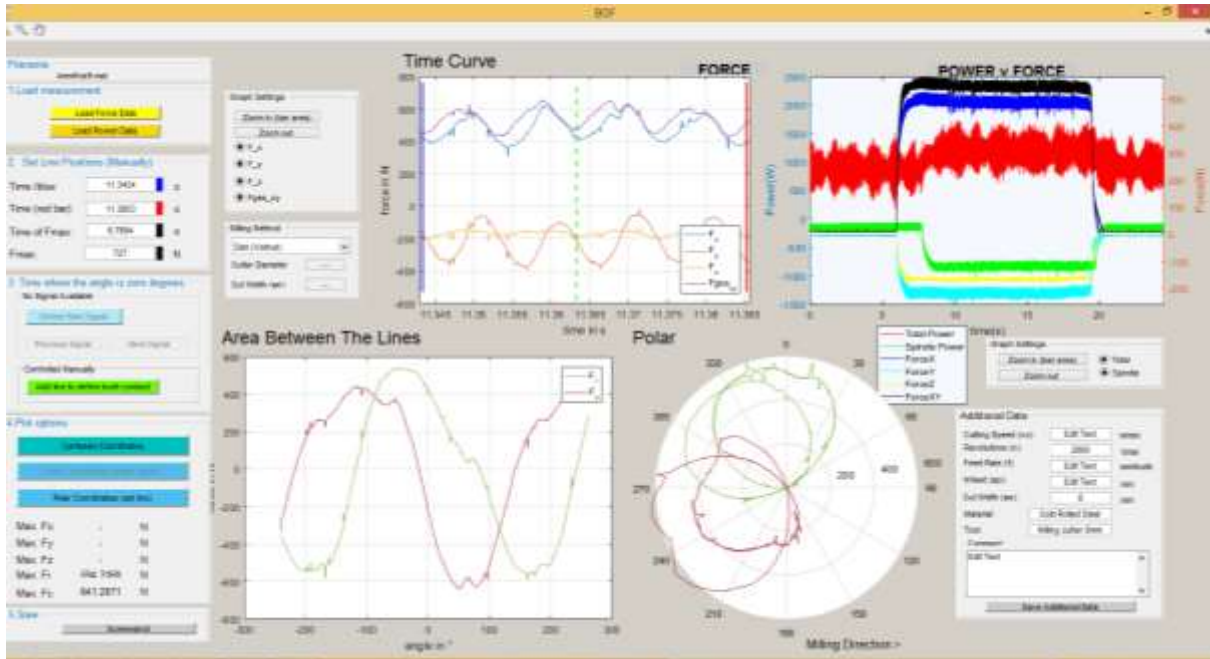


Figure 26. Initial Modification to the Force Interface, Source: Own contribution

The user interface is exported as an application (.exe) file which allows running the program on any Windows computer without the need of MATLAB. The objective is to install the app in the MMC of the DMG MORI machine and to demonstrate how data are uploaded and further analyzed in the machining place.

### 6.2.2 User Interface practice

Once the application is opened it is shown an initial interface like in Figure 27. After clicking the “Start New Analysis” button, the window selection option appears with the options: “Force vs Power”, “Force vs Force”, and “Power vs Power”.



Figure 27. Initial Appearance of the Interface and selection of new type of comparison, Source: Own contribution

After selecting the type of comparison, it will be asked to the user to select the correspondent data. If the selected data does not have specific properties of the file like a time vector or a starting date of measurement, a “wrong file” message will appear on the screen until the right data is selected.

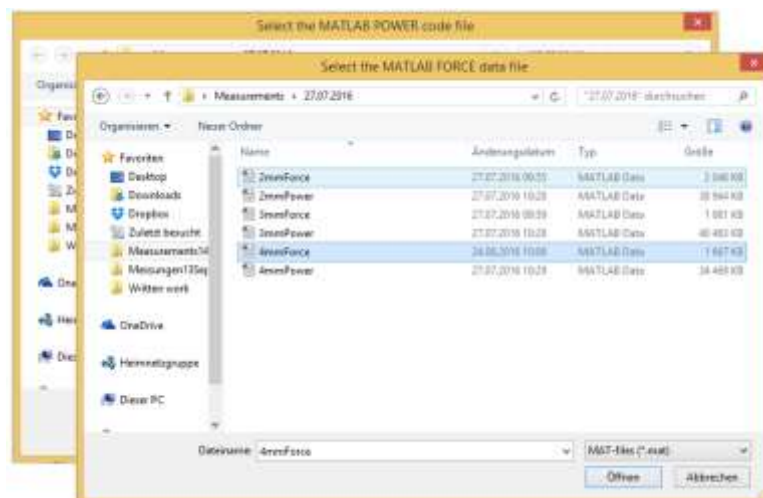


Figure 28. Data Upload for Force vs Power Comparison, Source: Own contribution

Depending on the selected type of analysis, the further steps, calculations, plots and other elements vary.

Power and force values have very high oscillations. When evaluating force, it is important to check the highest force values that the tool suffers, that way the life of the tool can be properly checked. A function which identifies peaks within a time interval was used. The force line shows the join of the highest force during a revolution for the whole process.

A moving average function was used for the power plotting since the user identifies the energy consumption as the area below the power curve and therefore is the moving average the best representation although very high peaks and also very low values are measured.

### 6.2.4 Force and Energy

Here the power elements can be renamed according to the measurements. There is an automatic recognition according to the most commonly measured variables. The one with the highest average power values will be assigned to the total machine variable and the one left to the spindle (see Figure 29). If this is not the case, the user can rename them.

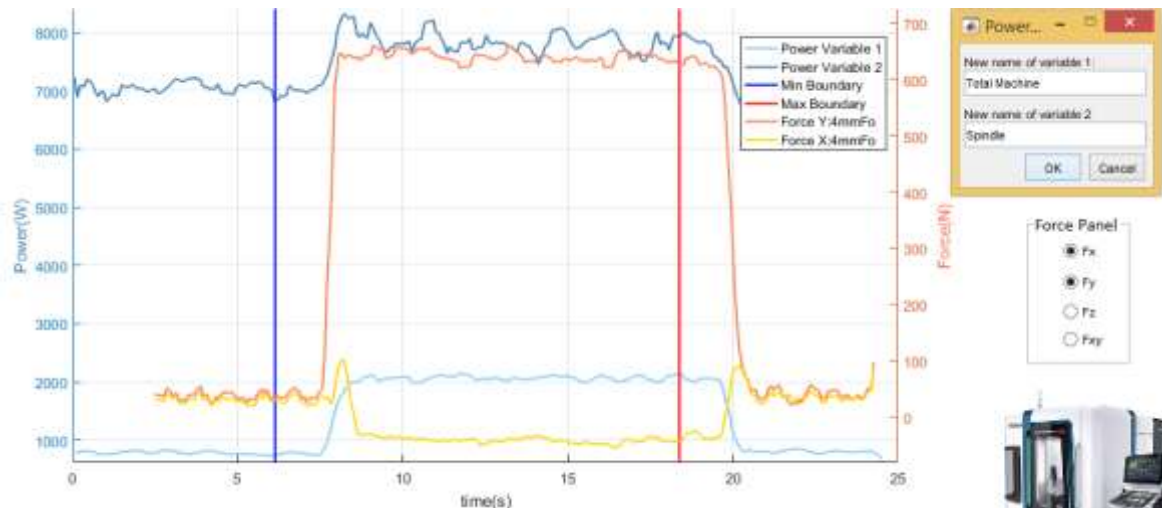


Figure 29. Power Variables renaming, Source: Own contribution

In this example, the total machine power and the spindle power were measured. The Variable1 in (dark blue) is identified and renamed as the total machine. Consequently, variable 2 corresponds to the spindle values.

After the renaming is completed, the interface calculates the most important factors of the process, according to the range between the minimum boundary (blue line) and maximum boundary (red line), defined by the user by dragging the lines to establish the beginning and end of the machining or any other interesting range of the process. These calculated variables are shown in the upper part of the interface (see Figure 30).

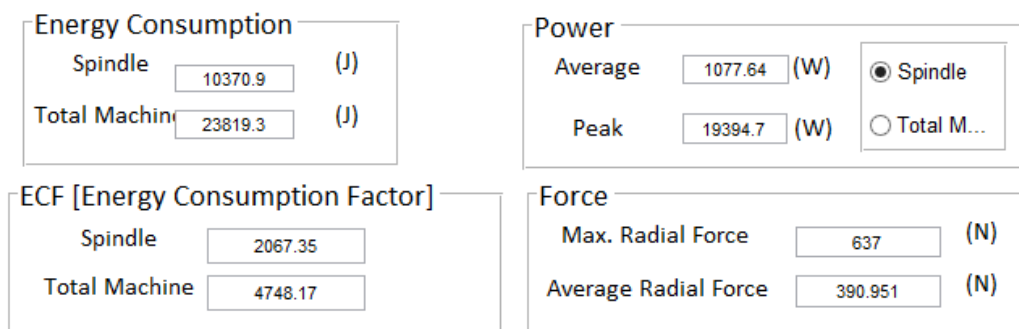


Figure 30. Machining Process relevant data, Source: Own contribution

Energy consumption, energy consumption factor, average and peak power; maximum and average cutting force are calculated according to the boundaries set by the user. If the user wants to focus on the start of the machining point, that section should be in the chosen range.

The most relevant data of the test are shown in a table (see Figure 31) located on the upper right side of the user interface. The material, tool, number of teeth, method, tool diameter, cut width, axial depth, feed rate, rotational speed, cutting speed and the maximum forces reached for X,Y and Z. Also, the XY maximum force is shown.

Some of the variables estimated in Figure 30 cannot be calculated if some information is missing from the experiment. Therefore, a slight modification of the force data acquisition software from Ewald Grabner should be done so the file could only be saved once all the information had been filled in. Some additional information like method and tool diameter should be included into the force data acquisition software.

	Value	
	Value	
Material	ST52	
Tool	Mill 16 mm	
Number of Teeth		2
Method	Up-Milling	
Tool Diameter / mm		16
Cut Width $a_e$ / mm	3.2	
Axial Depth $a_p$ / mm	2	
Feed Rate $F$ / mm.rev <sup>-1</sup> )	0.1	
Revolutions / min <sup>-1</sup> )		2984
Cutting Speed / m.min <sup>-1</sup>	150	
Max Force X / N		637
Max Force Y / N		293
Max Force Z / N		288
Max Force XY / N		638

*Figure 31. Table with cutting process parameters and other relevant data, Source: Own contribution*



### 6.2.5 Energy Consumption Factor

The Energy Consumption Factor is a non-dimensional number developed at the Production Engineering Institute which intends to establish a relation between consumed energy during machining  $E$ , the cutting volume  $V$ , and specific force  $k_c$ . It gives a machine or a specific process a determined value and allows classification and comparison.

$$\mathbf{ECF} = \frac{\mathbf{E}}{\mathbf{v} * \mathbf{k}_c} \left[ \frac{\mathbf{N} \cdot \mathbf{m}}{\mathbf{m}^3 \cdot \frac{\mathbf{N}}{\mathbf{m}^2}} \right] \quad [6-14]$$

The energy consumption factor has the potential to measure the energy efficiency for specific processes, machine subsystems, or a whole machine tool. When evaluating for example the total energy consumed by a machine, in order to do a face-mill of a constant volume of material  $v$  for a defined material with a specific force  $k_c$ , and then comparing it to the energy consumed by a second machine tool, a lower value would represent a higher energy efficiency.

The same process can be done to determine the best parameters for a machining process. A simple example: A company which produces specific parts need to face mill 2 mm depth of cold rolled steel. The two options possible varying the depth of cut are to do a single mill of 2 mm or a double pass machining, milling 1 mm per step. The energy consumption of both processes is measured and then the ECF values are compared. Finally, the most energy efficient (lower ECF) method is chosen.

The user of the interface determines the machining timeframe (blue and red line shown in the plot). According to that selection, the total energy consumption is calculated as the integral over the time of the power. The machined volume is the product of the length of cut, depth of cut and the cut width.

Normally, the value of the specific force  $k_c$  is obtained from multiplying diverse factors which include material properties, cutting velocity, an angle of cutting, conditions of contact between workpiece and inserts, and many others. In this case,  $k_c$  is obtained from an experimental approximation, explained in detail in section 7.2.

$$\mathbf{k}_c = \frac{\mathbf{F}_c}{\mathbf{A}} \text{ in } \frac{\mathbf{N}}{\mathbf{m}^2} \quad [6-15]$$

For the ECF calculation, the specific force value should be in metric units, which means that the area has to be calculated in meters. In the same manner, the removed volume has to be calculated in cubic meters although it might seem like a very small value.

The  $k_c$  approximation works for a number of inserts equal or inferior to two. To be able to determine  $k_c$  in all the possible cases, it is necessary to implement a sensor that establishes the exact point of at least one cutter. This would allow the exact calculation of the cutting force  $F_c$ .

Then, a theoretical input developed by J. Heikkala would be implemented, which means that the real area in contact at a time could be calculated and therefore a specific force value for a multiple cutters mill can be precisely determined.<sup>21</sup>

The initial angle of contact  $\varphi_{min}$  and the angle when a tooth stops making contact with the workpiece  $\varphi_{max}$  would be identified. The central position of the tool  $y$ , the tool diameter  $D$ , and the width of the workpiece  $a_r$  are parameters for identifying these angles.

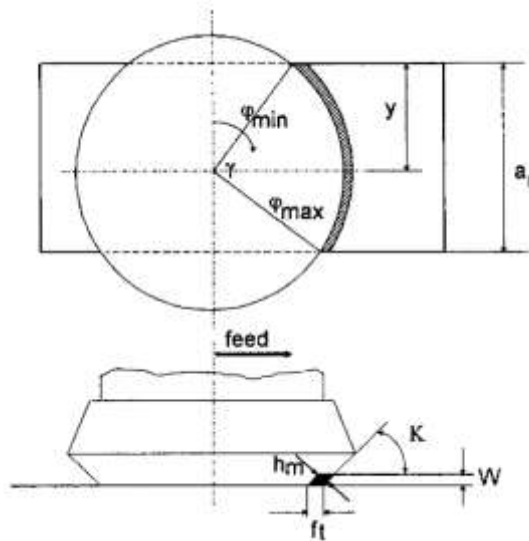


Figure 32. Geometry in face milling: Process angle determination, Source: Heikkala, 1995 p. 5

$$\varphi_{max} = \frac{\pi}{2} - \arcsin \frac{2y}{D} \quad [6-16]$$

$$\varphi_{min} = \frac{\pi}{2} + \arcsin \frac{2(a_r - y)}{D} \quad [6-17]$$

<sup>21</sup> Heikkala, 1995

Process angle  $\gamma$

$$\gamma = \varphi_{max} - \varphi_{min} \quad [6-18]$$

Number of teeth in contact simultaneously

$$k = \frac{\gamma \cdot z}{2\pi} + 1 \quad [6-19]$$

With the number of teeth in contact, the total cross-section area would be then the multiplication of  $k$  and the area contact of each tooth with the workpiece.

### 6.2.6 Force vs Force

After the selection of the force vs force option, the interface will ask the user to load the first force data file. An image like the following (Figure 33) will be shown in a smaller plot. Since the length of the recorded time and the start point of the machining are different for both force files, the user should drag a green line and approximately define a start point for the machining. This point should be clear and easy to identify. However, it depends on the depth of cut and the width of cut how heavily the force increases. For deeper milling processes, the start of the machining point is easier to identify. The user can also introduce a number under the label “Minimum Point”. Finally, a simple Ok is needed to set the point. Then the second force file is required to be loaded and the machining start point determination is required.

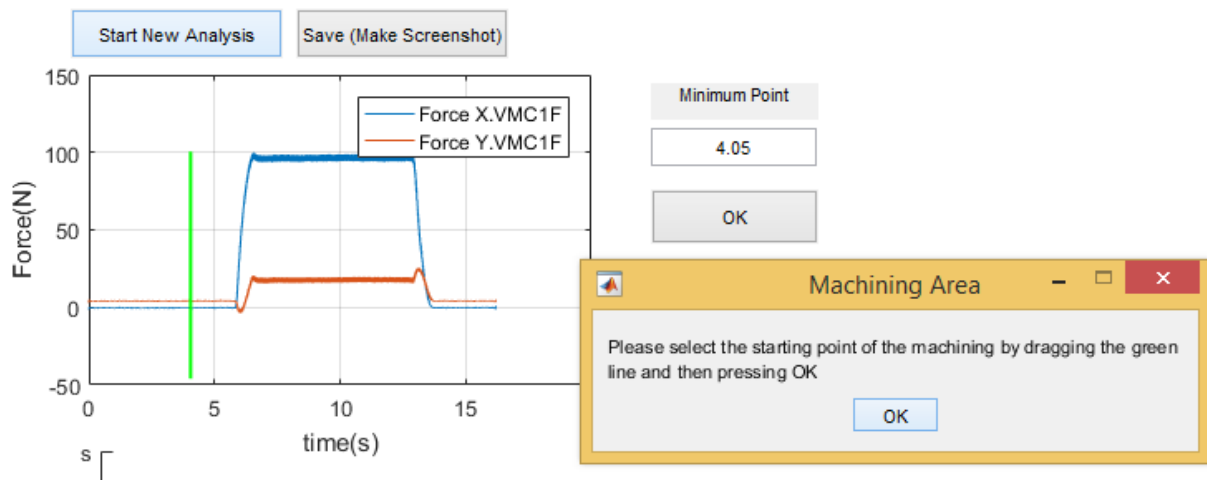


Figure 33. Plotting of independent force data and selection of start of machining, Source: Own contribution

Following the machining start point selection, the forces will be displayed in the bigger plot. The color similarity makes easier to identify the plotted forces and to compare the same variable from one data file to another (see Figure 34). The sketch on the right side of the interface shows the coordinate system and the feed direction for both down-milling and up milling.



Figure 34. Force vs Force Interface, Source: Own contribution

The cutting force is also calculated regarding the method. It is to mention that the value is an approximation to the average of the highest forces for each revolution during the machining time. Therefore, the blue and red lines are shown, so the user can also establish the exact time frame to calculate the different variables. The right side check buttons allow the user to show or hide a specific force variable (X,Y,Z,XY).

A maximum of two variables can be shown at a time, which means, 4 plot lines. The legend specifies the name of the variable and is followed by the first part of the file name, so the user can identify them. On the top right corner, a table like in the first force vs power comparison is shown, but in this case it includes the relevant information for both tests.

### 6.2.7 Energy vs Energy

Loading the data files works similar to the force vs force option. A similar starting point has to be chosen. However, the start of the machining point is harder to identify in this case and therefore is recommended to the user to select the peak before machining which represents the start of the spindle rotation (see Figure 35).

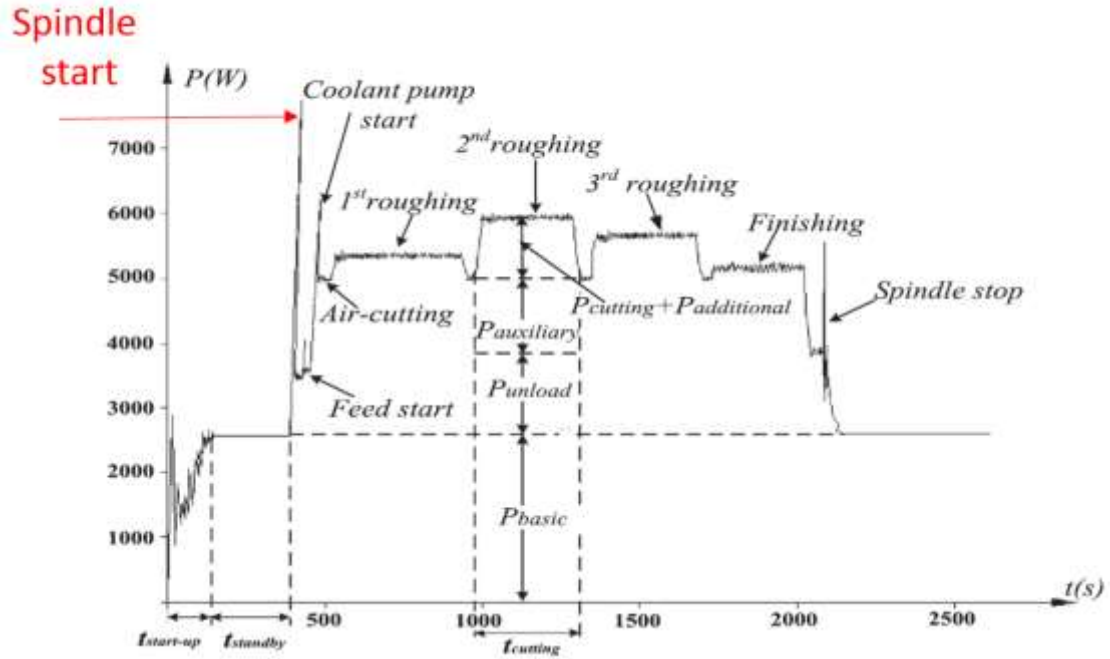


Figure 35. Power profile of a multi-pass CNC milling, Source Li, et al., 2016 p. 3

The figure above shows the power profile for a multiple step milling. In our case of study, only one pass test was carried out. In this case, the power profile looks like shown in Figure 36

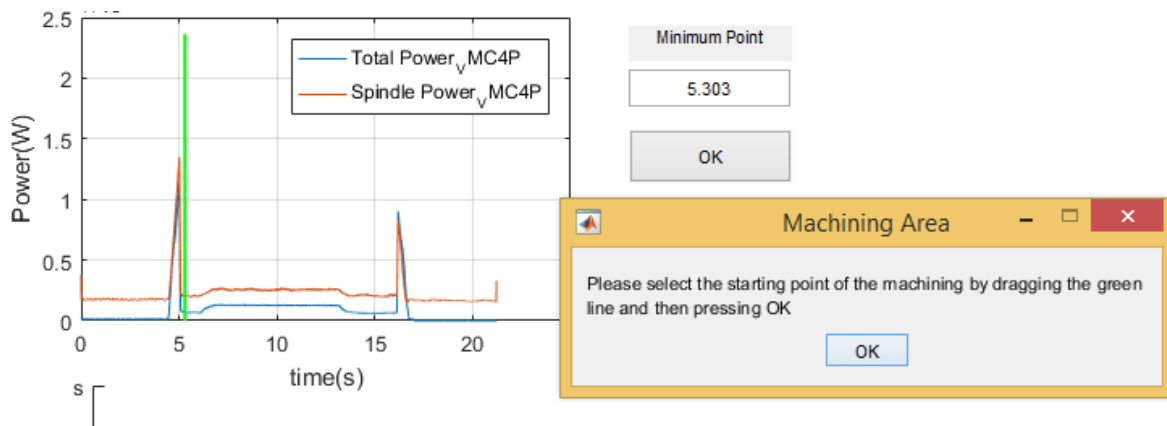


Figure 36. Power profile of a single-pass CNC milling, Source. Own contribution

Similar to the force vs force comparison, the interface will plot both data files and the average power and the peak power values are shown.

### **6.2.8 Saving**

After the data analysis, the user has the option to save it. A screenshot of the plot is created according to a user's given name and automatically an excel file in the same folder with the most relevant data of the analysis is generated.

Stored data: material, tool, tool diameter, number of teeth, method of cutting, cut width, axial depth, feed rate, rotational speed, cutting speed, maximum force (x,y,z,xy), energy consumption, average and peak power, energy consumption factor.

### **6.2.9 Further development**

For the Energy vs Energy Analysis, it would be desirable to run a complete process, including feed displacements with no machining, tool changes and of course the machining step. The same procedure should be run for different machine tools and the energy consumption results would be then valid for comparing energy efficiency.

## 7 Experiments and Results

### 7.1 Power Measurement Settings

For this project, the power measurements focused on the most relevant process data groups within a machining process:

- Total machine power
- Spindle power

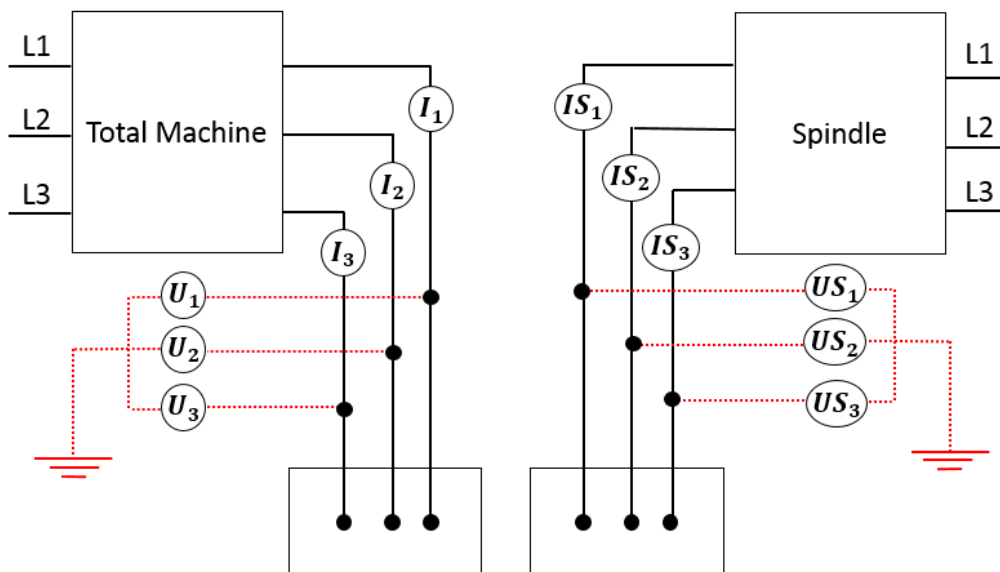


*Figure 37. Equivalent Circuit Diagram of the Power Measurement*

The specific connection points can be found in Appendix 3. Since the current and voltage were measured for all three phases for both spindle and total machine, all the 12 channels were busy. It is to mention that a different connection is possible reducing the number of channels from 6 per data group to 4. If that is applied to both data groups, 4 channels would be free to measure the third device (e.g. cooling pump, X, Y,Z,B,C axes; Tool magazine, etc.) In that case, a modification to the interface code is necessary since the data acquisition files would change and therefore the power calculation.

The DMG Mori Spindle Motor Module specifications (see Appendix 2) has a rated pulse frequency of 4 kHz. Considering the Nyquist-Shannon sampling theorem (see page 7) measurements with a sampling frequency (SF) of 10 kHz are carried out and a Fourier transform done. Figure 38 shows the frequency spectrum for the spindle in the DMG Mori Machine.



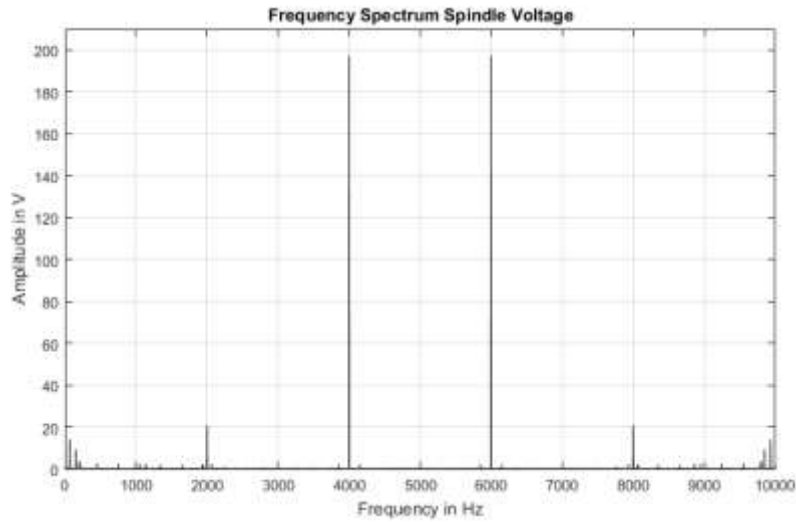


Figure 38. Frequency Spectrum for Spindle Voltage (SF:10kHz), Source: Own contribution

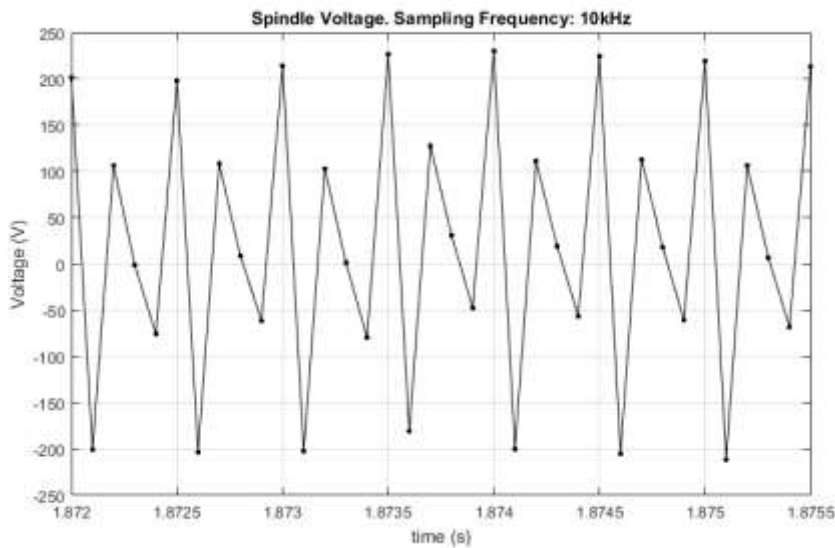


Figure 39. Spindle Voltage Time domain (SF: 10 kHz), Source: Own contribution

It is seen in Figure 38 that the frequency of which the most relevant data is found is 4000 Hz. However, since the range of the sampling frequency is only 10 kHz, it could happen that important data over 5000Hz is lost and the evaluation might incur in under-sampling.

Figure 39 shows the voltage in the time domain. The signal does not follow a sinus behavior and it is clearly under-sampled. The range of sampling frequency for the power measurements can be up to 1MHz. Unfortunately, when using such a big sampling rate, the amount of data stored is too high and the processing time for the computer increases significantly.

The optimum power sampling value had to be found with a practical approach. First, by measuring the voltage and current with a much higher sampling frequency (200 kHz).

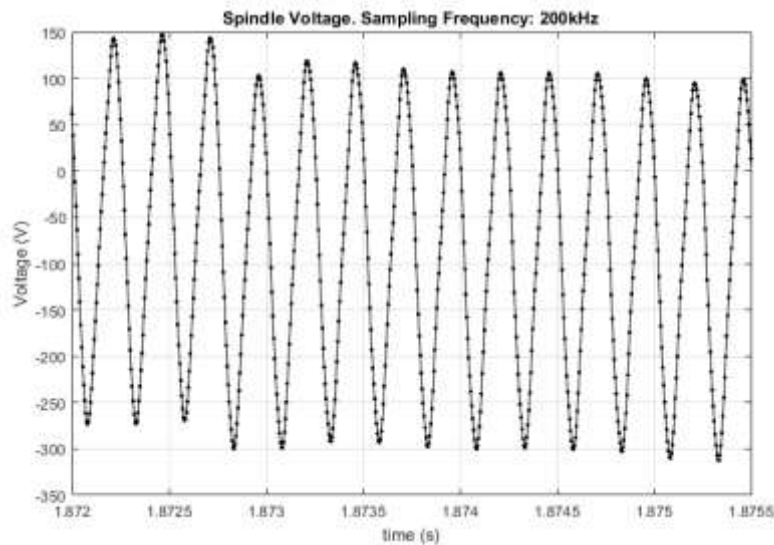


Figure 40. Spindle Voltage Time domain (SF: 200 kHz), Source: Own contribution

In Figure 40 the voltage signal is much clearer and as expected it follows a sinus wave. It is probable to have acquired all the relevant signals and that can be checked at the frequency spectrum.

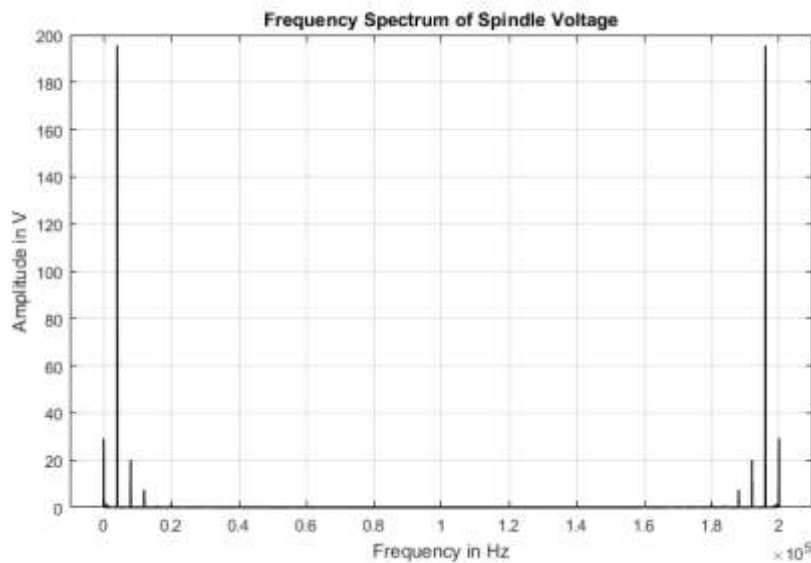


Figure 41. Frequency Spectrum for Spindle Voltage (SF:200kHz), Source: Own contribution

All the important data seem to be stored but in order to find an optimal and less memory consuming sampling frequency, the instantaneous power is calculated and after the energy consumption. This data will be stored as  $E_{200kHz}$ . Then using Matlab, data with SF of 50 kHz will be obtained by taking every fourth point of the initial measurement. The same procedure but taking every tenth data point will make a current and voltage signal of only 20 kHz. The

same power and energy calculations are done and finally a relation between them and the initial  $E_{200kHz}$  (see Table 5).

Axial Depth $a_p(mm)$	Cut Width $a_e(mm)$	Cutting Speed $v_c(m/min)$	Rotational Speed $N (rpm)$	Material
5	10	0.1	2000	SAE 1020

Table 4. Properties of the cutting test for a Power sampling rate of 200 kHz

Measured time: 74.12 seconds

Figure 42 shows the voltage measured signal for the different sampling frequencies. Both 200 kHz and 50 kHz signal show a clear and smooth wave. At 20 kHz, the signal becomes less clear but at the peaks can be recognized. For lower frequencies, the signal form is not consistent and the original signal is not clear to identify. The data is proven with the information at the Table 5. The total power consumption difference is very low (less than 0.03%) for a SF=20 kHz.

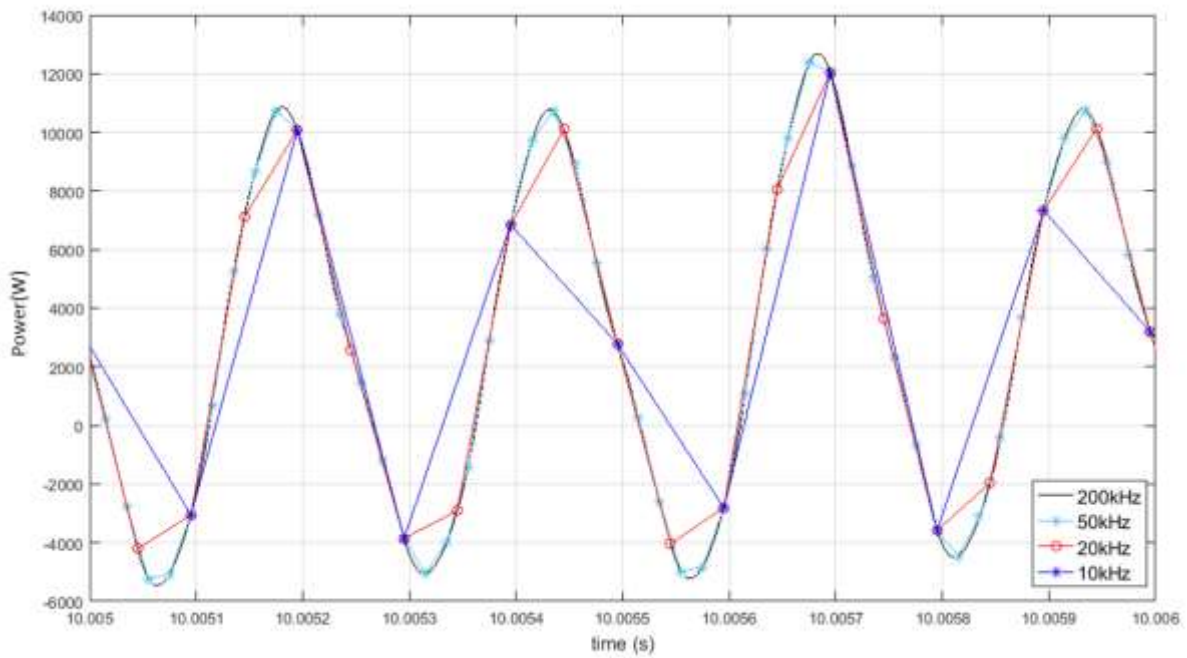


Figure 42. Power measured at different sampling rates, Source: Own contribution

Sampling Frequency	Average Power	Total Consumed Energy	$\left(\frac{E_x}{E_{200kHz}} - 1\right) * 100\%$
200 kHz	141.18 W	1046.5 kJ	-
50kHz	141.19 W	1046.6 kJ	0.0039
20kHz	141.14 W	1046.2 kJ	0.0282

Table 5. Differences in the power and energy calculations for SF=200 kHz, 50 kHz and 20 kHz

Configuration of the parameters into DEWESOFT Software (Figure 43 and Figure 44):

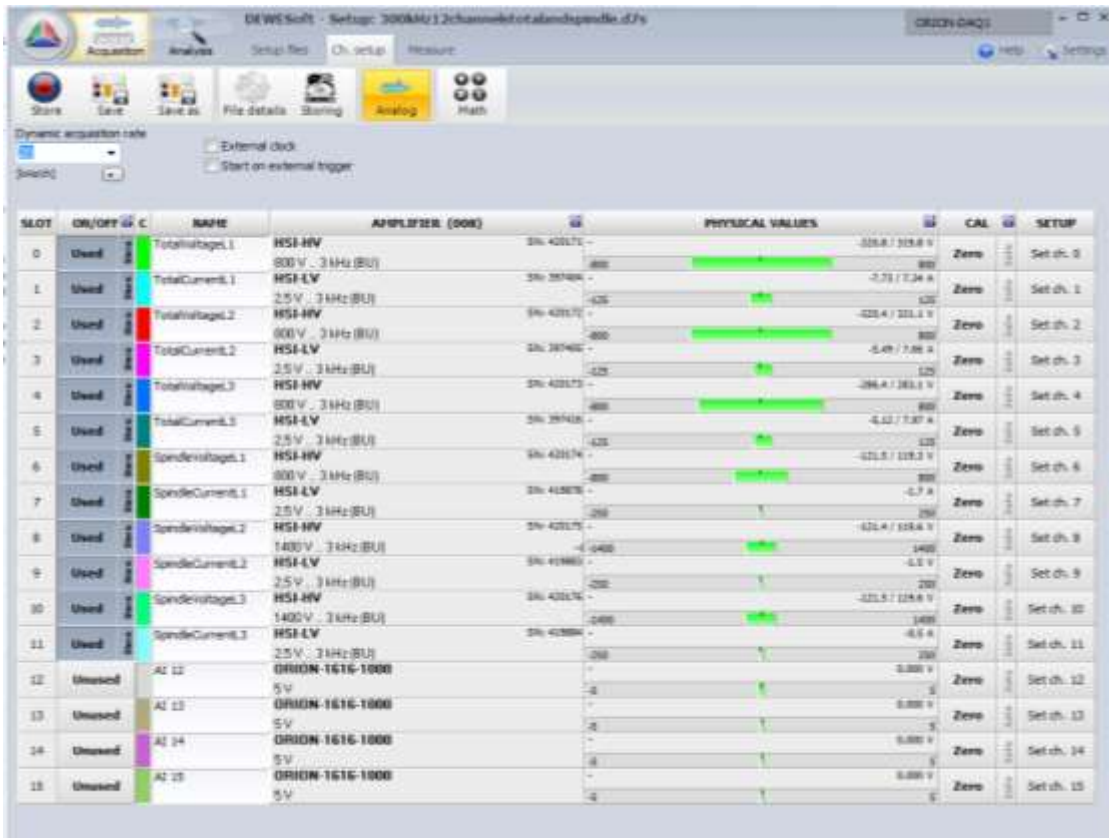


Figure 43. Channels Set-Up for the DEWESOFT Software. 12 Channels, 20 kHz Sampling frequency, Source: Own contribution

The current channels configuration depends on the type of amplifier used. The voltage channel configuration depends on the range for the specific sub-system measured.

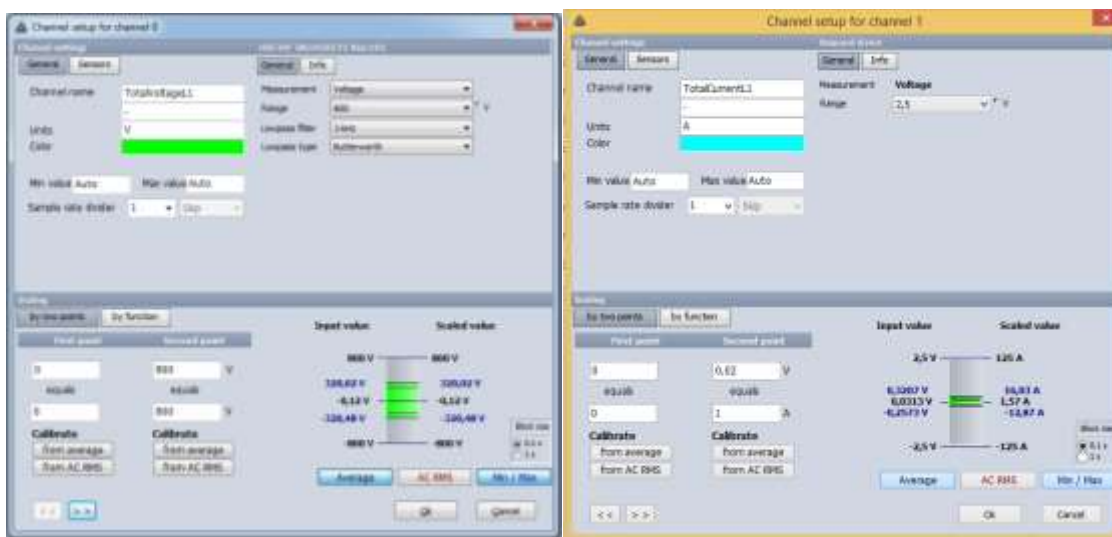


Figure 44. Left: Voltage channel configuration, Right: Current channel configuration, Source: Own contribution

## 7.2 Specific Force $k_c$ determination

$k_c$  is established as the relation between cutting force  $F_c$  and the cutting cross-section  $A$ .

Since the force  $F_c$  depends on the direction of cutting (up-milling or down milling, see Figure 45), two approximations have to be done. The cross section area and the force  $F_c$  change over the time. For this case of study, and therefore, for the code of the interface, the higher force  $F_c$  case possible will be taken for the  $k_c$  value.

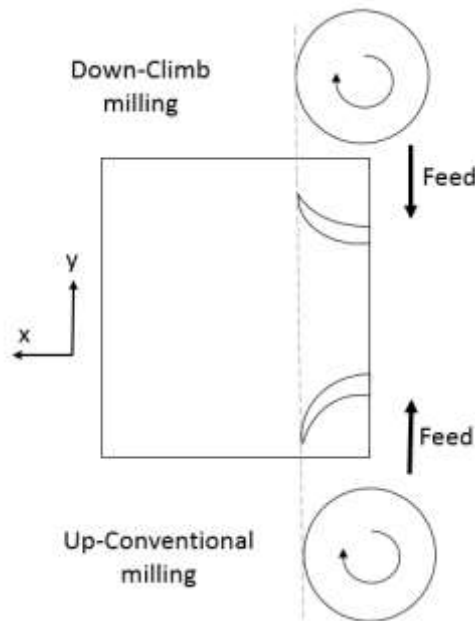


Figure 45. Up and Down milling, Source: Own contribution

### 7.2.1 Conventional milling (Up-milling)

As seen in Figure 45, the chip width starts at zero and it increases over the time. It causes more heat to diffuse into the workpiece.

#### Cutting Force $F_c$

Depending on the cutting point, the value of  $F_c$  changes and can be practically found by recognizing the specific starting point of one revolution during the machining, setting it as the  $\varphi = 0^\circ$  point, converting the time vector into an angle vector (rotational speed needed), and applying the matrix formula [4-11] for each angle point. In the left side of Figure 46, the green line represents the start of the cutting in one revolution. Since it was only a one tooth mill, the cutting happens only during the first  $180^\circ$ .

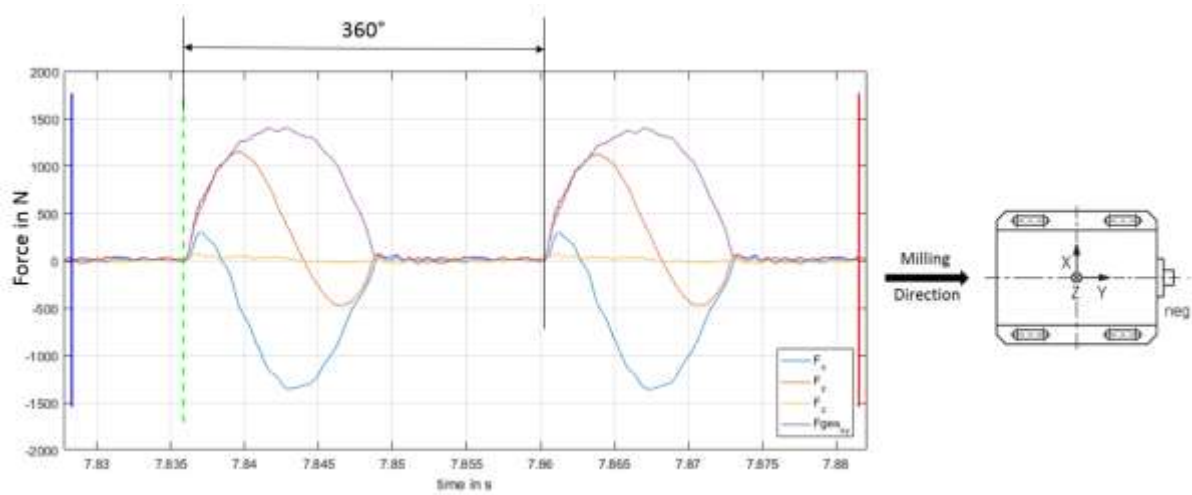


Figure 46. Left: Time Curve of Forces for a full slot test, Right: Cutting Force at a specific angle  $\varphi$ ,  
Source: Grabner, 2016

Several tests were carried out to find out a pattern of the behavior of  $F_c$  and its relationship with  $F_x$  and  $F_y$ . Figure 47 shows the cutting force during one revolution of a one tooth full slot milling test. When the angle  $\varphi = 90^\circ$ ,  $F_c$  reaches its maximum value. For a milling tool with a number of teeth superior to 2, the cross-section also changes during one revolution.

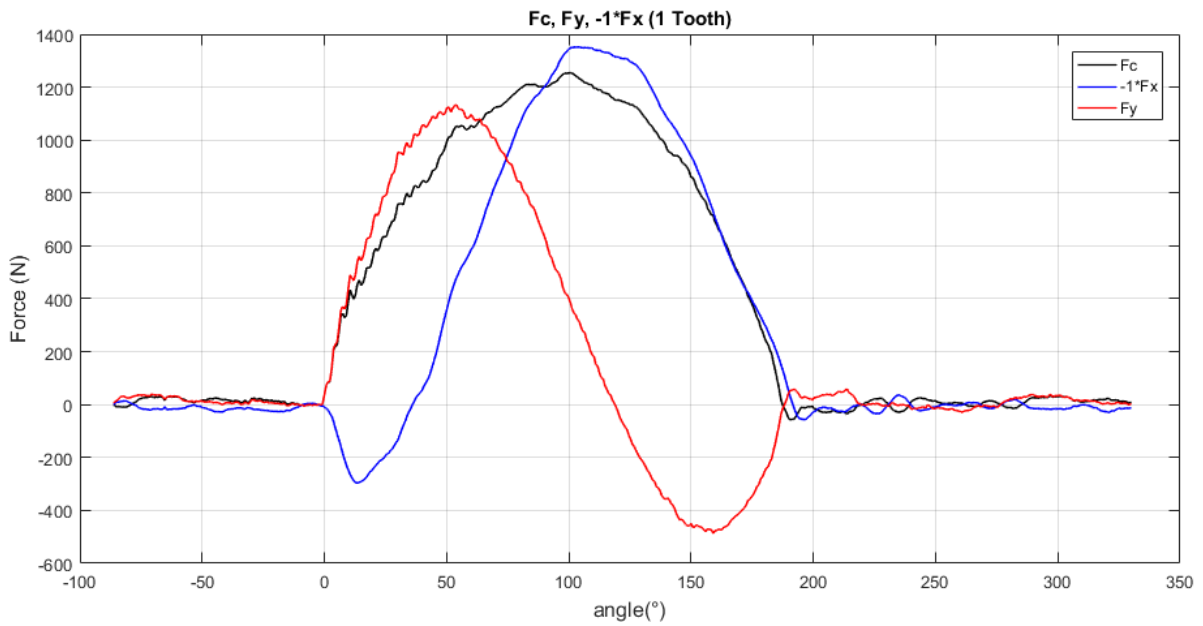


Figure 47.  $F_c, F_x, F_y$ : One Tooth, VMC 600 Machine,  $a_e=25$  mm,  $a_p=5$  mm, Full Slot

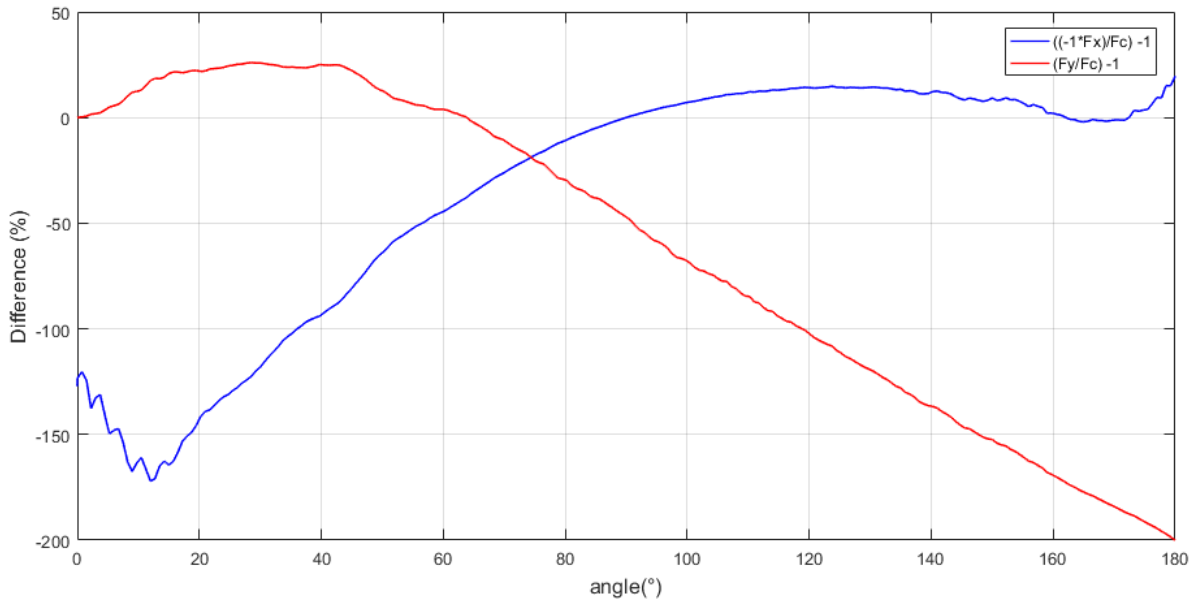


Figure 48. Difference (in Percentage) Between  $F_c$  and  $F_x, F_y$

Although the plot in Figure 47 looks very similar to what theory establishes, not all the tests behave the same way and depending mostly on the depth of cut and the cut width, the forces  $F_y, F_x$  and therefore  $F_c$  have more vibrations. For a test with a lower  $a_e$  and  $a_p$  values like the one shown in Figure 49 the force has many oscillations.

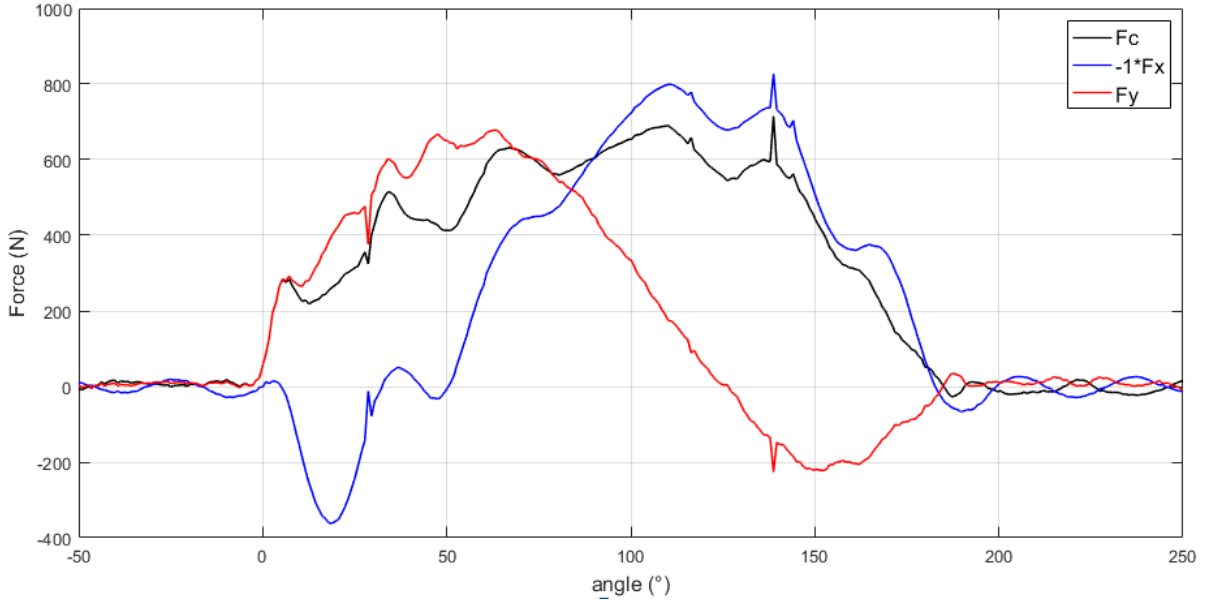


Figure 49.  $F_c, F_x, F_y$ : One Tooth, VMC 600 Machine,  $a_e$ :16 mm,  $a_p$ : 3mm, Full Slot

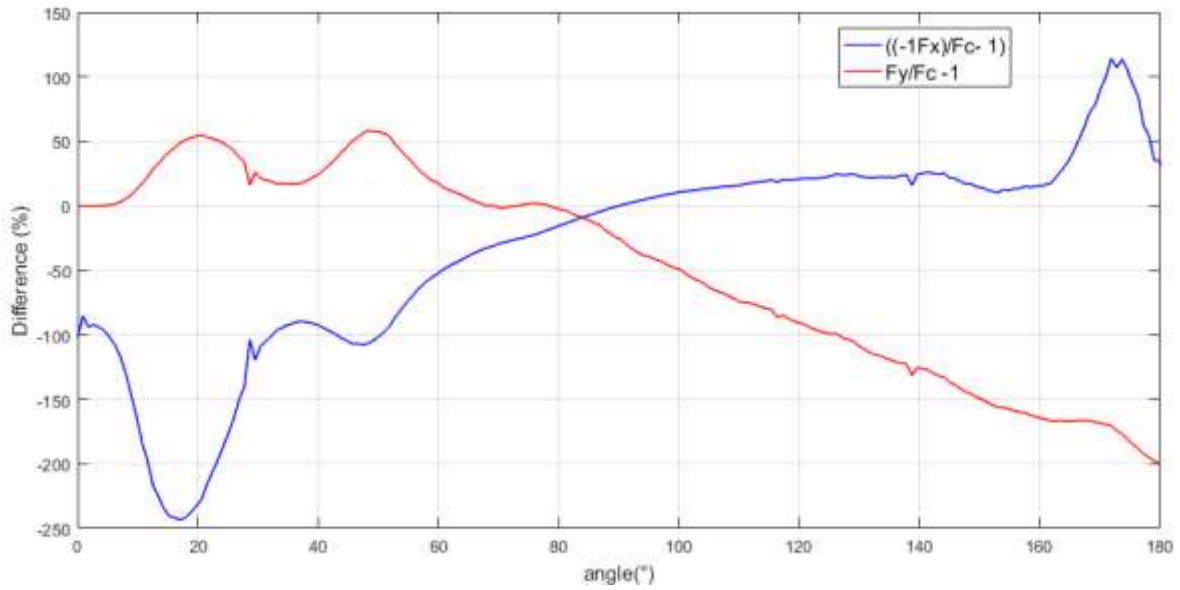


Figure 50. One Tooth Difference (in Percentage) Between  $F_c$  and  $F_x, F_y$

A deeper analysis was done in order to determine the best approximation of  $F_c$  to  $-F_x$  or  $F_y$ . Table 6 shows the angle where both  $F_y$  and  $-F_x$  meet for several milling tests, carried out for full slot milling. Before the meeting point,  $F_c$  is more similar to  $F_y$  and after it, to  $F_x$ .

Test	Meeting Angle $\varphi$ $F_y = -F_x$ (°)	# of Teeth	$a_p$ (mm)	Machine
21D	75,3	1	2	DMG
41D	73,2	1	4	DMG
21V	83,51	1	2	VMC 600
41V	82,4	1	4	VMC 600
22D	77,3	2	2	DMG
42D	77,7	2	4	DMG
22V	81	2	2	VMC 600
42V	80,95	2	4	VMC 600

Table 6. Opposite direction full slot milling tests to determine angle  $\varphi$  when  $F_y = -F_x$

Material	Milling Tool Diameter (mm)	Cutting Speed $v_c$ (m/min)	Feed per tooth $f_z$ (mm)	Overlap
ST52	16	150	0,1	100%

Table 7. Relevant further test parameters for  $k_c$  tests



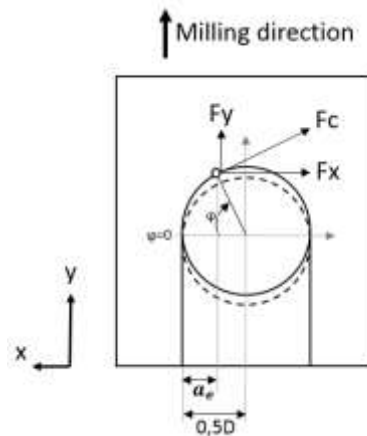


Figure 51. Forces diagram and angle  $\varphi$ , Source: Own contribution

$$\varphi = \arccos\left(1 - 2\frac{a_e}{D}\right) \quad [7-20]$$

$$a_e = -\frac{\cos \varphi - 1}{2} \quad [7-21]$$

Average meeting angle  $\varphi$ :  $79^\circ$

Overlap where  $F_c \sim -F_x$ :  $a_e \geq 0,4D$

### Cutting Cross Section A

The cutting cross section A is a product of the wide of the thickness  $h$  and the chip width  $b$ . The chip width is dependent on the sinus of incidence angle  $\kappa$ :  $b = a_p / \sin \kappa$ .

For this project all the tools used have an incidence angle  $\kappa$  of  $90^\circ$  and therefore  $b = a_p$ <sup>22</sup>.

$$A = b \cdot h = a_p f_z \sin \varphi \quad [7-22]$$

If the overlapping is inferior to 50% the cutting cross-section will be calculated with the formula [7-22]. Otherwise, as the highest force happens at 50% ( $\varphi = 90^\circ$ ) overlapping or near it, the cutting cross-section is  $A = a_p f_z$ .

### Resume for the software:

If the overlap is smaller than 40%:  $F_c = F_{y_{max}}$

If the overlap is higher than 40%:  $F_c = F_{x_{max}}$

If the overlap is higher than 50%:  $A = a_p \cdot f_z$

If the overlap is lower than 50%:  $A = a_p f_z \sin \varphi$

<sup>22</sup> Eberhard, et al., 2008 p. 220

### 7.2.2 Climb (Down) milling

The chip width has its maximum value at the beginning and then decreases. Generated heat is primarily transferred to the chip. It is nowadays the commonly used milling process.

#### Cutting Force $F_c$

Like shown in Figure 52, the maximum cutting force and the maximum chip thickness are close to an overlapping angle  $\varphi = 90^\circ$ .

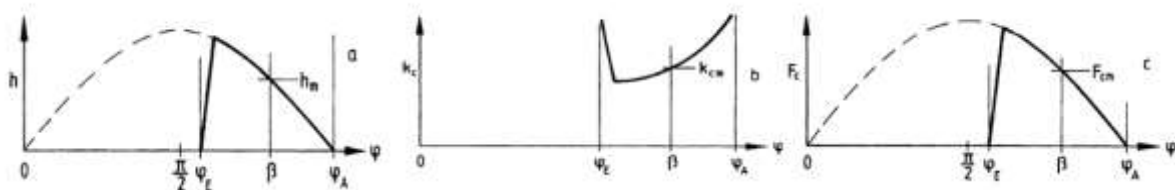


Figure 52. Chip thickness (left), specific force (middle), and cutting force (right) for one tooth climb-milling, Source (Eberhard, Sven, Marco, & Franz, 2008, p. 215)

The cutting force curve is very similar to the  $F_x$  curve and therefore the approximation  $F_c \sim F_{x_{max}}$  is acceptable. To prove this assumption, several tests were carried out for different overlap values. The data has been further analyzed and the calculation of  $F_c$  has done following the equation matrix [4-11].

The idea of the approximation is to reduce complexity of the interface. The user doesn't have to look the data into detail selecting a specific cutting start and run the force equation matrix. In Figure 53, where a 50% overlap test is shown.

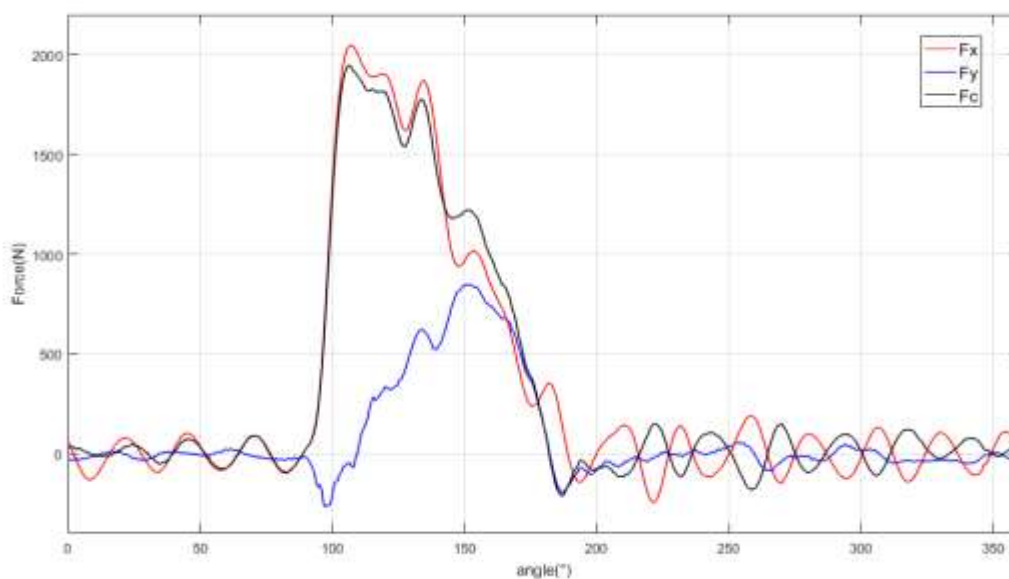


Figure 53. Forces in X and Y axis and cutting force  $F_c$  for a 50% overlap climb-milling, Source: Grabner, 2016

A test with an overlap of 10% is shown in Figure 54. Here, the forces  $-F_x$  and  $F_c$  show a very similar behavior at the machining period, which goes from angle  $\varphi = 144^\circ$  until  $\varphi = 180^\circ$ .

The parameters for all the following climb-milling tests shown:

Cutting speed: 200 m/min

Feed Rate: 0,25 mm/tooth

Depth of cut: 5 mm

Machine tool: DMG Mori Ultrasonic 30 linear

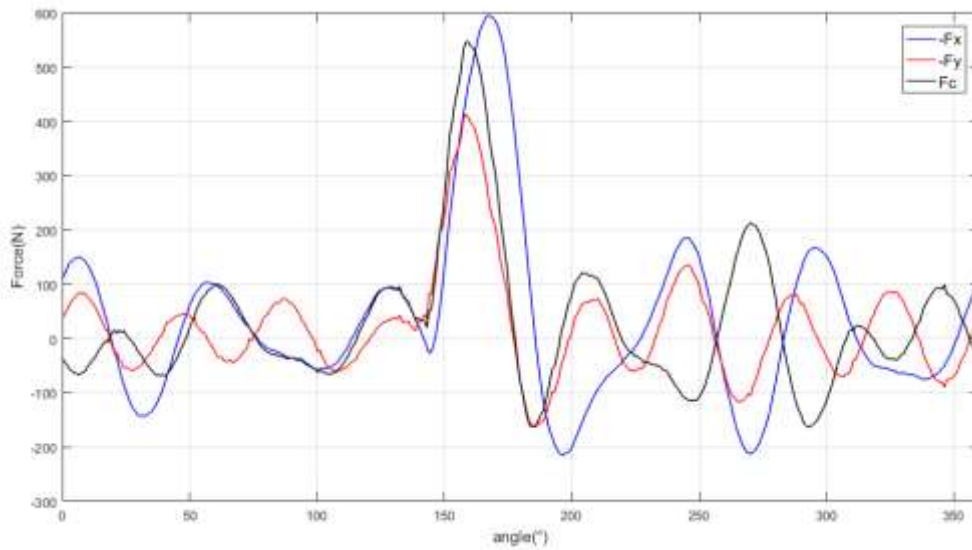


Figure 54. 10% overlap. Climb-milling, Source: Own contribution

Two more tests have been done for different overlap values: 75% and 25% the idea behind them is to prove that the approximation is valid for different overlap values.

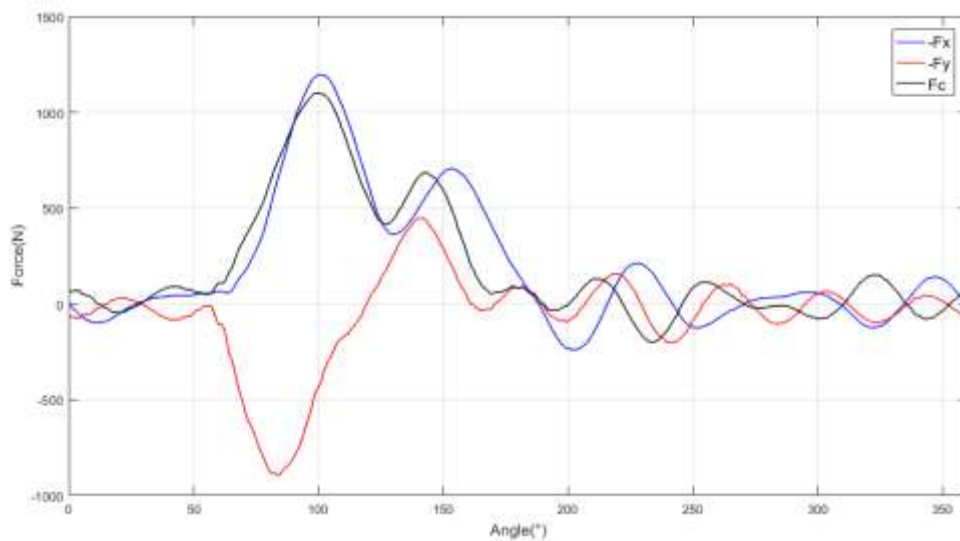


Figure 55. 75% Overlap. Climb-milling, Source: Own contribution

For a 75% overlap, the forces  $F_x$  and  $F_c$  have a very similar behavior. It has to mentioned that the most relevant similarity is for this case where the angle is close to 50% because at this point the highest force values are expected and the cross-cutting section is at maximum. For this case, when  $\varphi = 90^\circ$ ,  $F_c = 1010$  N and  $F_x=1045$  N. For an overlap of 25% is the only case where the difference between  $F_c$  and  $F_x$  is considerable and the assumption wouldn't be valid. At the highest value for  $F_x$  ( $145^\circ$ ) = 1182 N, the cutting force  $F_c$  ( $145^\circ$ ) = 730 N.

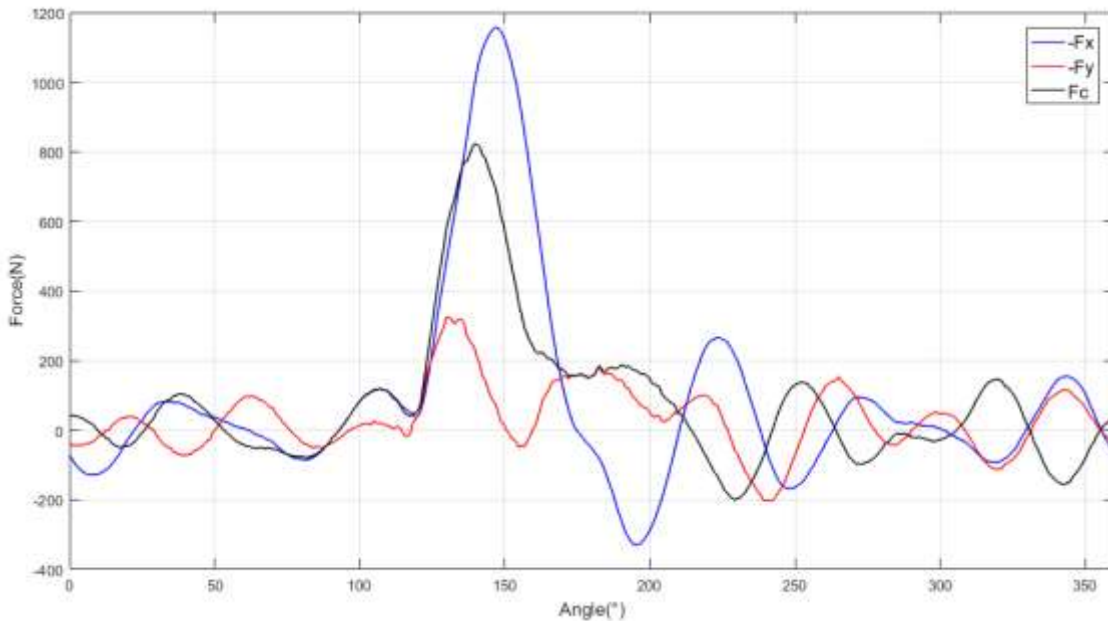


Figure 56. 25% overlap. Climb-milling, Source: Own contribution

### Cutting Cross Section A

For an overlap equal or superior to 50%, the maximum cutting force is obtained near the  $\varphi = 90^\circ$  point and therefore an approximation of the cross section is calculated like:

$$A = b \cdot h = a_p f_z \sin \varphi = a_p f_z \quad [7-23]$$

For an inferior overlap to 50%, the cross section is calculated the same way as for the conventional milling. First, the angle  $\varphi$  is calculated from the cut width and then the area based on the formula [7-22].

Resume for the software:

$$F_c = F_{x_{max}} \quad [7-24]$$

If the overlap is higher than 50%:

$$A = a_p \cdot f_z \quad [7-25]$$

If the overlap is lower than 50%:

$$A = a_p f_z \sin \varphi \quad [7-26]$$

To prove the results of the specific force calculations, a comparison with the real data found in handbooks should be done. As shown in Figure 57, the specific cutting force should be around 1.5 and 2.8 MPa for a milling of steel when the depth of cut is superior to 1mm. Polishing, grinding and rubbing have higher specific forces but therefore the depth of cut is much lower (from  $10E^{-5}$  to  $10E^{-2}$  mm).

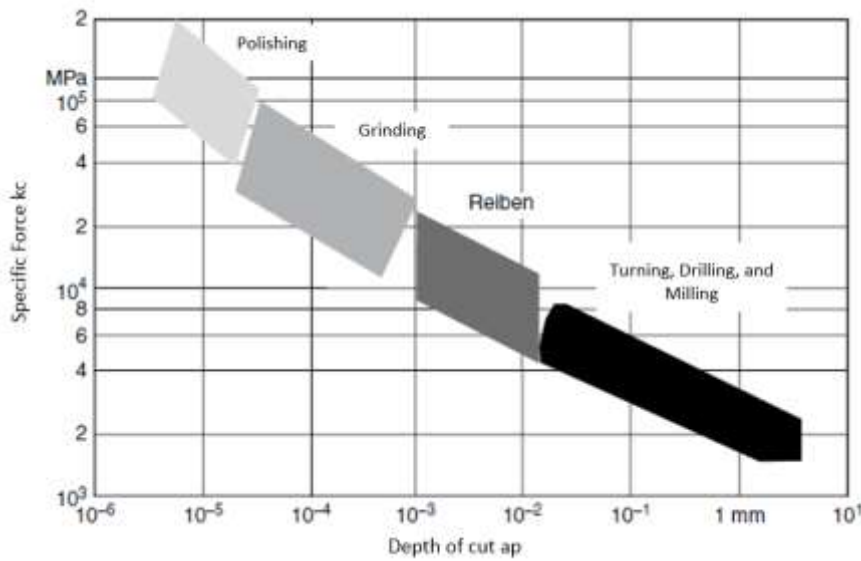


Figure 57. Specific Cutting Force and Cutting depth for steel, Source Berend, et al., 2011 p. 55

### 7.3 Tools and Machines

Two different machine tools available at the Institute of Production Engineering were used for the power and force measurement tests.

**Machine Tools:**

	<b>DMG Mori Ultrasonic 30 Linear</b>	<b>EMCO VMC 600</b>
<b>Controlling System</b>	CELOS - SIEMENS	Heidenhain TNC 426
Working area (X,Y,Z)	320 / 300 / 280 mm	1200 / 410 / 360 mm
<b>Spindle Drive</b>		
Power (100/40% duty cycle)	15,2 / 19,5 kW	7,5/11 kW
Rotational Speed range	20-40.000 1/min	0-6000 1/min
Maximum Torque	16	95N.m
<b>Feed drive</b>		
Drives	Linear (X,Y,Z) Servomotor (B,C)	Linear (X,Y,Z)
Feed rate (X,Y,Z)	Linear: up to 50.000 mm/min B: 50 rev/min, C: 100 rev/min	0,01 – 12.000 mm/min
Rapid motion (X,Y,Z)	50 m/min	Max. 24 / 24 /18 m/min
Feed force (X,Y)	-	Max 5.000 N
Feed Force (Z)	-	Max 8.000 N
Resolution	0,01 $\mu\text{m}$	0,001 mm
<b>Tooling System</b>		
Maximum tool weight	120 kg	5 kg
Maximum tool diameter	70 mm	(100 next to 40 mm)all 63 mm
Maximum tool longitude	220 mm	220 mm
<b>Electrical connection</b>		
Power Supply	3/PE ~400V	3/PE ~400V
Frequency	50/60 Hz	50/60 Hz
Max. Voltage fluctuation	-	+5/-10%
Connected Load	-	20 kVA
Back-up fuse	-	35 A

*Table 8. Technical Data of the machine tools, Source EMCO MAIER GmbH, 1998, SAUER GmbH, 2015*

Three different cutting mills were used. Tool number 2 (Table 10) has initially 4 teeth and after some teeth were grinded to compare the measurements for 2 teeth and 1 tooth behavior.


Tools:

<b>#1</b>	<b>OSAWA G2410</b>
Diameter	8 mm
Number of teeth	4
Material	Hard metal

*Table 9. OSAWA mill relevant data*

<b>#2</b>	<b>Mill 16 mm</b>
Diameter	16 mm
Number of teeth	4
Material	Hard metal

*Table 10. 16 mm Mill relevant data*

<b>#3</b>	<b>BOEHLERIT</b> <b>ISO 90 P</b>	 <p><i>Figure 58. ISO 90P Source: (BOEHLERIT, 2016)</i></p>
Diameter	16	
Number of teeth	1 or 2	
Cutting Insert	BCP35M	
Insert Material	Hard metal	

*Table 11. Boehlerit Mill 16 mm relevant data*

7.4 Test Methodology and Parameters

Machine Tool	DMG MORI 30 Linear	DMG MORI 30 Linear
Tool	#1	#2
Cutting speed (m/min)	50	30
Feed rate (mm)	0,2	0,2
Rotational speed (rev/min)	2000	600
Axial Depth (mm)	2,3,4	2
Method	Full slot	Full slot
Number of teeth	4	4,2,1

Table 12. Full Slot measurements parameters

Machine Tool	<ul style="list-style-type: none"> <li>○ DMG MORI 30 Linear</li> <li>○ EMCO VMC 600</li> </ul>
Tool	#3
Cutting speed (m/min)	150
Feed rate (mm)	0,1
Rotational speed (rev/min)	2984
Axial Depth (mm)	<ul style="list-style-type: none"> <li>○ 2</li> <li>○ 4</li> </ul>
Method	Full slot Conventional-Milling
Cut Width $a_e$	<ul style="list-style-type: none"> <li>○ 3,2</li> <li>○ 8</li> <li>○ 16</li> </ul>
Number of teeth	<ul style="list-style-type: none"> <li>○ 1</li> <li>○ 2</li> </ul>

Table 13. Different machine tools measurement parameters

Figure 59 shows the set-up of the workpieces for the tests. The different depth of cut can be seen. The Kistler measuring device is also shown holding the workpiece. Figure 60 shows the machine tools surface where the workpiece is attached to. The spindle tool can also be seen.





Figure 59. Milled workpiece with different depths of cut, Source: Own contribution



Figure 60. Left: DMU Setup, Right: EMCO VMC600 Milling Setup, Source: Own contribution.

## 7.5 Force and Energy

A force and energy analysis allows the identification of critical process steps. The objective of this work is to recognize the correlation of parameters and how the most relevant information can be visualized.

A typical curve for a force-energy relation plot should seem like the following:

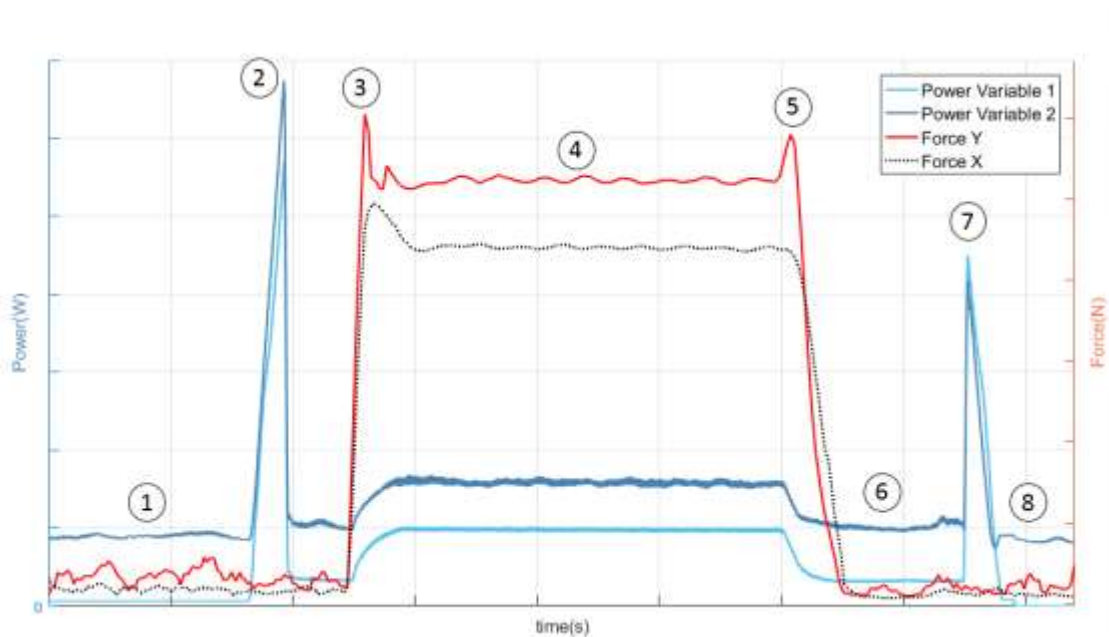


Figure 61. Power and Force typical plot for milling

It is important to know that the data obtained from the measurement devices does not look exactly like the plot. The raw data has very high oscillations and it is important that this one is filtered, so the noise is eliminated and a clearer behavior of the signal can be seen. There are 8 stages in this plot. The beginning of the curve (1) shows the forces and the spindle power with values close to zero, it is called as the stand-by state. Since the machine is on, some power load is present. The peaks (2) and (7) shown in the power lines correspond to the start and stop of the spindle motor. For some measurements, this peak does not seem to appear, which means that the spindle was already rotating when the data measurement and storage started. In some other measurements, only the first peak is present, which means the data storage was stopped before the spindle drive stopped rotating.

Peak (3) indicates the force increase due to the start of cutting. It takes a while until the forces stop the high oscillations and reach status (4), an almost stable state of machining for both forces and power. When the machining step is almost finished there is a peak (5) of force and the power starts decreasing. During step (6), the spindle keeps rotating and advancing in the feed direction for a short period of time. The stand-by state (8) appears again when the main spindle stops and there is no translation in the feed direction.

It has to be mentioned that although this is the expected plot, in many cases it might vary due to the way the machining was programmed. Multiple measurements have been carried out by varying parameters e.g. cut width, axial depth and number of teeth. The idea behind these tests is to prove and verify the measurements.

In the next charts, various test results are shown and explained. In the title of the comparison the user can see which parameter has been changed from one measurement to the other. The rest of the test parameters remain constant.

### Comparison 1: Different Machine tools:

Method: Full Slot, Number of teeth: 2, Tool Diameter: 16 mm, Feed per tooth: 0.01mm, Cutting Speed: 150 m/min, Rotational speed: 2984 rev/min. Workpiece material: ST-52

Figure 62 shows the power and force plot for the test with the DMG-Mori machine tool. Before the spindle starts rotating, the machine has an average power of around 2700 W which corresponds to systems and components like internal cooling, lubrication, controlling (digital panel) and active sensors like laser position or door state. When the spindle starts rotating, a peak of about 6 seconds is seen and the tool starts its movement towards the workpiece. As soon as the peak force appears, the power requirement of the spindle increases until it reaches a value of 525 W. At the same time the total machine power increases from 2800 W up to 3700 W, which means not only the spindle increased the total power requirement but also other aggregate that needs around 200 W.

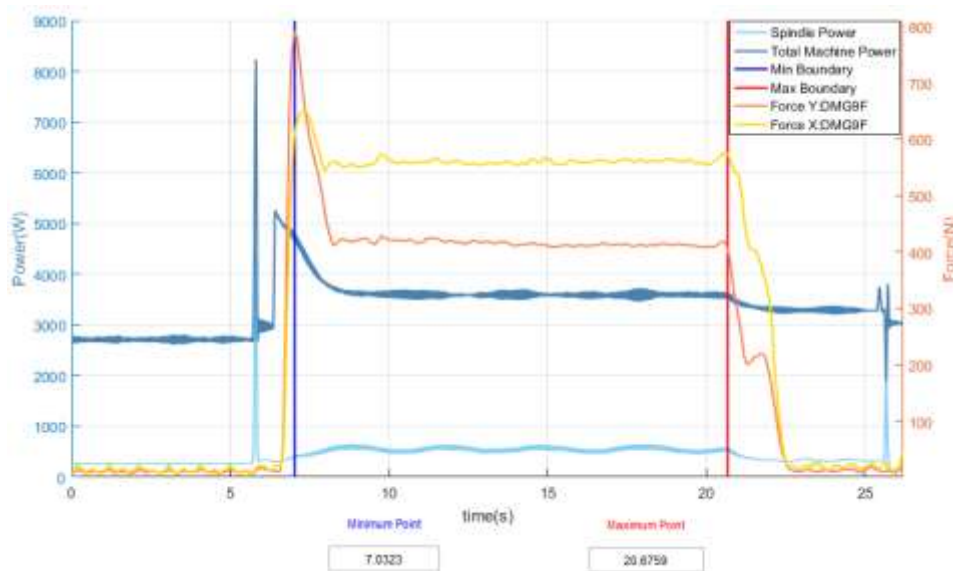


Figure 62. DMG MORI Force and Power Milling

Comparing the power requirement of the DMG machine to the EMCO VMC-600 during the standby state, the first one needs around 800 Watts more. During the machining, the DMG machine requires 1500 Watts more than the VMC-600 (see Table 14). It has to be mentioned

that the spindle of the VMC-600 machine needs a power of around 1kW during the machining which is why the total power increases the same amount.

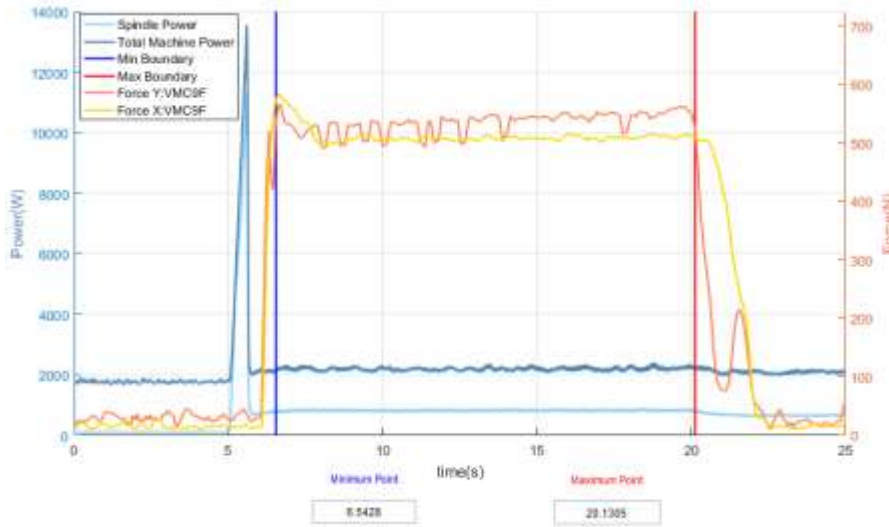


Figure 63. EMCO VMC600 Force and Power Milling

The maximum forces for both machines are similar. However, in the DMG machine the force in the X direction is lower than in the Y axis and for the VMC machine the values are very similar but  $F_x$  is almost always higher. Since the spindle power requirement of the VMC600 machine is almost twice as high as the DMG, the consumed energy of the VMC machine increases vastly. However, the total consumed energy for the machines shows that the DMG has many different aggregates running at the same time, for instance, the dust extractor, the spindle cooling or other. The energy consumption shows clearly the behavior of the components, which means, the spindle of the DMG has a lower ECF and therefore it is a more energy efficient component. However, when comparing the total machine, VMC-600 has an ECF of almost 12 compared to 16,6 of the DMG.

	DMG	VMC600
<b>Fc (N)</b>	558,77	501,75
<b>Max Force X / N</b>	654	588
<b>Max Force Y / N</b>	810	724
<b>Max Force Z / N</b>	210	218
<b>Energy Consumption Spindle (J)</b>	7160	13410
<b>Energy Consumption Total Machine (J)</b>	50392	32387
<b>Average Power Spindle (W)</b>	525	987
<b>Average Power Total Machine (W)</b>	3693	2384
<b>Peak Power Spindle (W)</b>	2820	18574
<b>Peak Power Total Machine (W)</b>	8754	23225
<b>ECF Spindle</b>	2,36	4,94
<b>ECF Total Machine</b>	16,61	11,94

Table 14. Relevant data for machine tool comparison

**Comparison 2: Change in the cut width  $a_e$**

The process was evaluated for two different percentages of overlap. The first one, with a 20% overlap, which means a cut width of 3.2 mm (the same tool was used). Its correspondent plot is shown in Figure 64. The forces behavior is rather different between the Y and the X direction. It is an expected result because the overlap is small which means the chip cut in every revolution is done mostly in the Y direction. For higher overlaps, it is expected to have a similar force X and Y values. Regarding the power requirement in the total machine, some aggregate has to slowly decrease its power need after the spindle is turned on and that is why a slow reduction is seen.

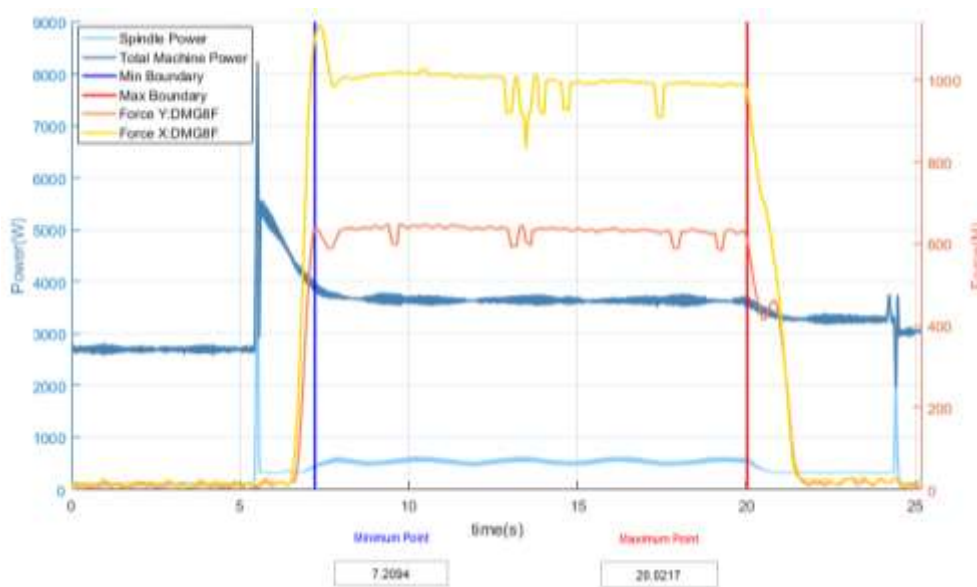


**Figure 64. 20% overlap force and power plot, Source: Own contribution**

The forces values for the 50% overlap are very similar, as expected. The peak values also indicate that the forces oscillate around 1000 N with the highest peaks at the beginning of the machining with average peak values of 1300 N but only during a short period of time. In this case, there is no aggregate for the total machine turning off slowly.

The numerical control program was identical to the 20% overlap test, which means that some components automatically go on and off. The machining time in both cases is the same since the number of teeth (1), the feed rate and the rotational speed are the same. In the first test (20% overlap) the power required by the spindle is around 500 Watts and for the second test it goes up to over 1000 Watts values.

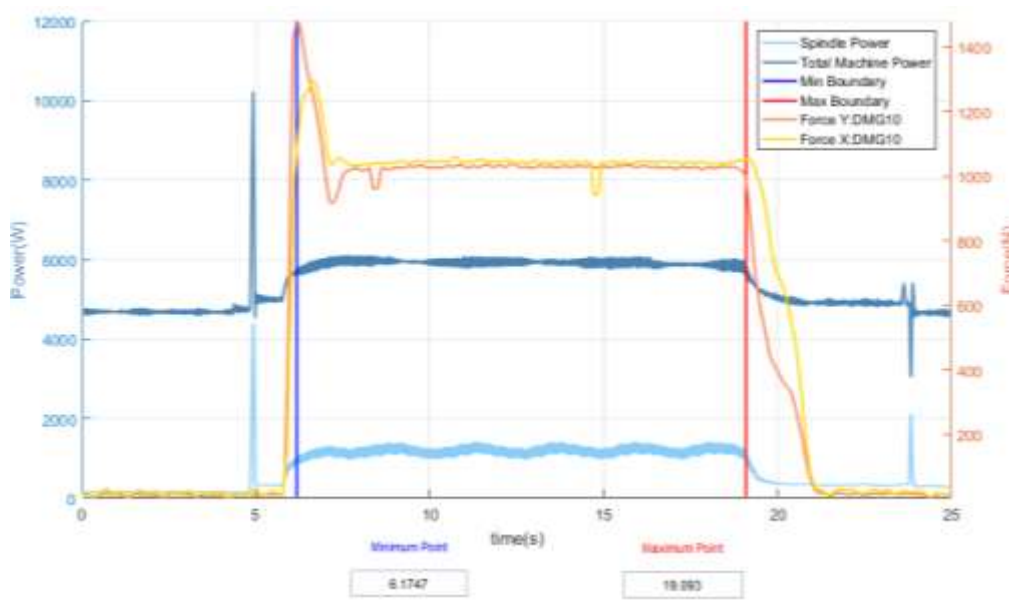


Figure 65. 50% Overlap force and power plot Source: Own contribution

The specific forces values are also very similar and close to the theoretical values which once again proves that the estimation is valid for these simple cases. The peaks of power are very similar going up to 15kW and the average power of the total machine is 45 % higher for the 50% overlap case. However, when looking at the spindle energy consumption factor, the 50% overlap case is more energy efficient, since the removed volume is much higher. The same happens when looking at the total machine ECF, where 13.46 corresponds to the 8 mm cut width and 24.66, almost twice the value of the 20% overlap test.

Overlap	20%	50%
<b>Cut width (mm)</b>	<b>3,2</b>	<b>8</b>
Max Force X (N)	1142	1310
Max Force Y (N)	654	1481
Max Force Z (N)	320	637
Max Force XY N	1145	1739
Machining time (s)	12,8123	12,9183
kc (N/mm <sup>2</sup> )	2416	2586
Energy Consumption Spindle (J)	6815	10685
Energy Consumption Total Machine (J)	48608	71385
Average Power Spindle (W)	532	827
Average Power Total Machine (W)	3794	5526
Peak Power Spindle (W)	11922	11985
Peak Power Total Machine (W)	14379	15856
ECF Spindle	3.458	2.01
ECF Total Machine	24.66	13.46

Table 15. Relevant data for cut width comparison

### Comparison 3: Change in the number of teeth $z$

For a full slot machining, and a depth of cut of 4mm, two tests were carried out with a number of teeth  $z = 1$  and  $2$ . Theoretically, the plots should look very similar in power and force value with a difference in the machining time, where the test with one tooth, should double the cutting time. The feed velocity is directly proportional to the number of teeth.

Figure 66 indicates that the machining time goes from  $t=4.8$  s until  $t=18.7$  s, for an approximate machining time of 13.8 seconds. For the two teeth test (Figure 67) the machining time is approximately 6.9 seconds which meets the expected results.

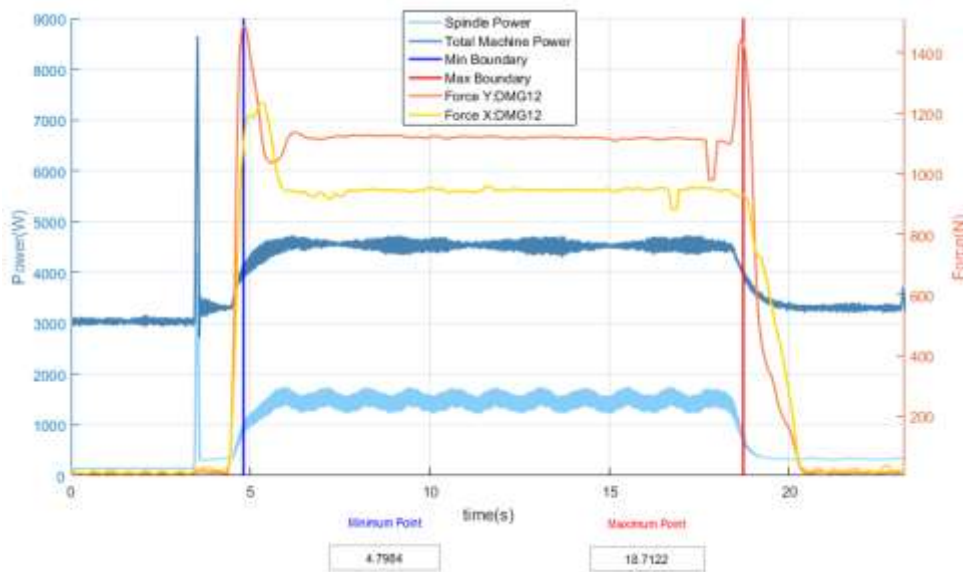


Figure 66 . One tooth 4 mm Depth of cut DMG, Source: Own contribution

The spindle power oscillates constantly during the machining period while the total power has a more stable behavior. Approximately the same amount of power that the spindle requires is the additional power that increases during the machining for the total power measurement. A different value would be seen as an error in the measurement. As mentioned previously, depending on the measurement all the different states would be seen. For the one tooth case, the data storage stopped before the spindle braked and therefore no power peak at the end of the plot is seen.

For the force variables, since the shown lines represent the union of the peak values for each revolution, it is also important to check the average forces. These values are taken from the excel file created when the analysis was saved.

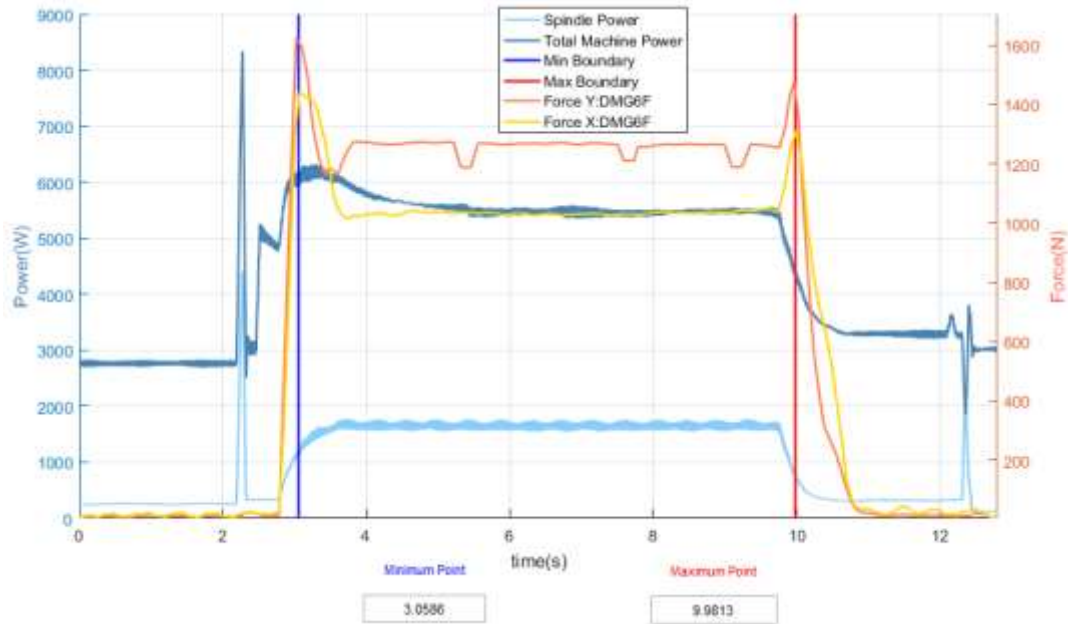


Figure 67. Two teeth, 4mm depth of cut, Source: Own contribution

The peak forces during the machining are similar for both measurements. The force in the X-axis is above 1200 N and for the Y axis there is a small difference: In the one tooth case, it is below 1000N and for the two teeth case it is above 1000N.

DMG		
Number of teeth	2	1
Machining time (s)	6,91	13,88
Average $F_x$ (N)	314,40	153,32
Average $F_y$ (N)	430,15	222,77
Fc (N)	1056	946
Energy Consumption Spindle (J)	8270	17257
Energy Consumption Total Machine (J)	33616	59582
Average Power Spindle (W)	1198	1243
Average Power Total Machine (W)	4868	4292
Peak Power Spindle (W)	12234	11881
Peak Power Total Machine (W)	12989	12906
ECF Spindle	0,713	1,651
ECF Total Machine	2,897	5,702

Table 16. Most Relevant data for number of teeth test comparison



Although the peak forces look quite similar in Figure 66 and Figure 67, the average forces vary strongly. When using two inserts the average forces in the X and Y axes almost doubles the single insert forces. The spindle power requirement is almost the same in both cases and the total power of the machine is higher for the two teeth case, but it is most probably related to another pump of an aggregate of the machine that was running at that time, which does not affect the milling process itself. On the other hand, the energy consumption of the spindle for the single insert is twice as big as the double insert test. The lower ECF value for the two teeth test also proves that this method is much more efficient in terms of energy.

Comparison 4: Change in the depth of cut  $a_p$

For this tests, two inserts were used for an overlap of 20%. The depth of cut was doubled for the second test so the differences could be clearly seen. The machine tool was the EMCO-VMC600.

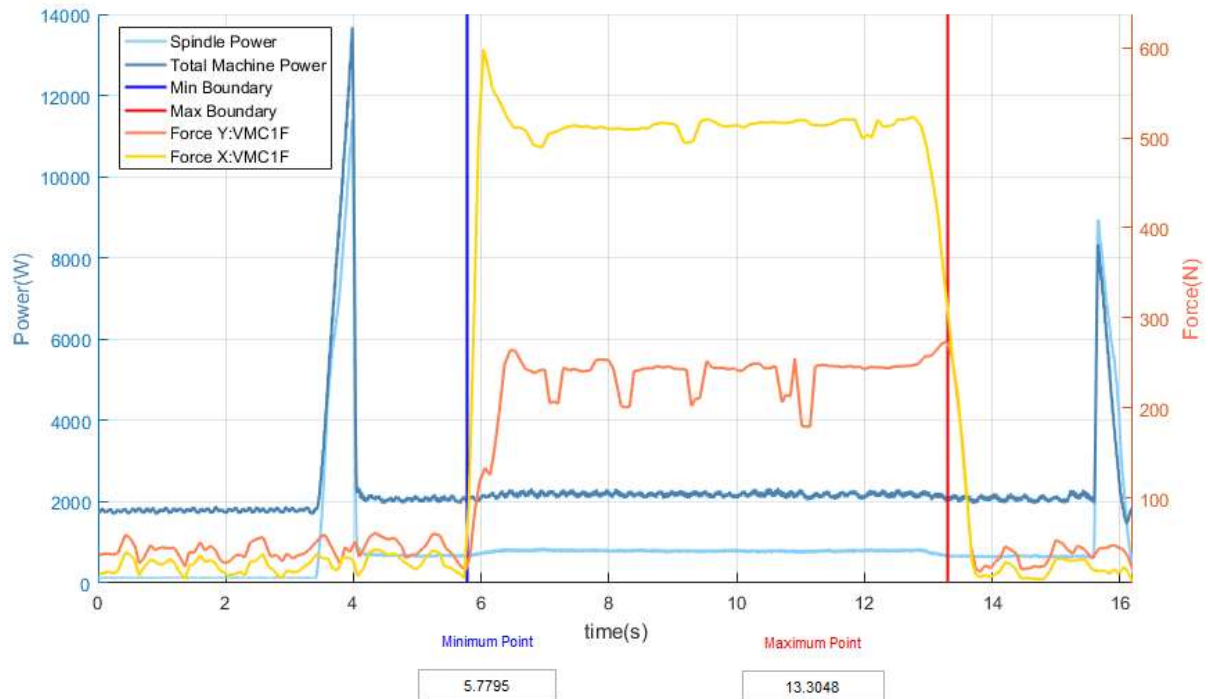


Figure 68. 2 mm depth of cut test, Source: Own contribution

As a short mention to the power plot, the user cannot state that the highest peak value corresponds to the actual peak value from the raw data. The moving average function does not allow high oscillations during very short periods to affect the plot, which is convenient for a general view purpose. However, the user can not underestimate the power requirements of the machine according to the peaks shown on the plot and that is the reason why the peak power values are exported into the Excel file when the “Save” button is clicked.

For the force plots there was also a moving average used but in this case, the time span between the averaged points is shorter because the expected values from the peaks recognition should not vary as much as the power data. This happens during the machining which is why the force curves look very stable between the blue and red lines. The same does not happen to the previous state, where no real force data should be felt by the machine bed but due to the rotation of the spindle and probable noise waves and vibrations it could generate, the measurement devices shows high oscillations.

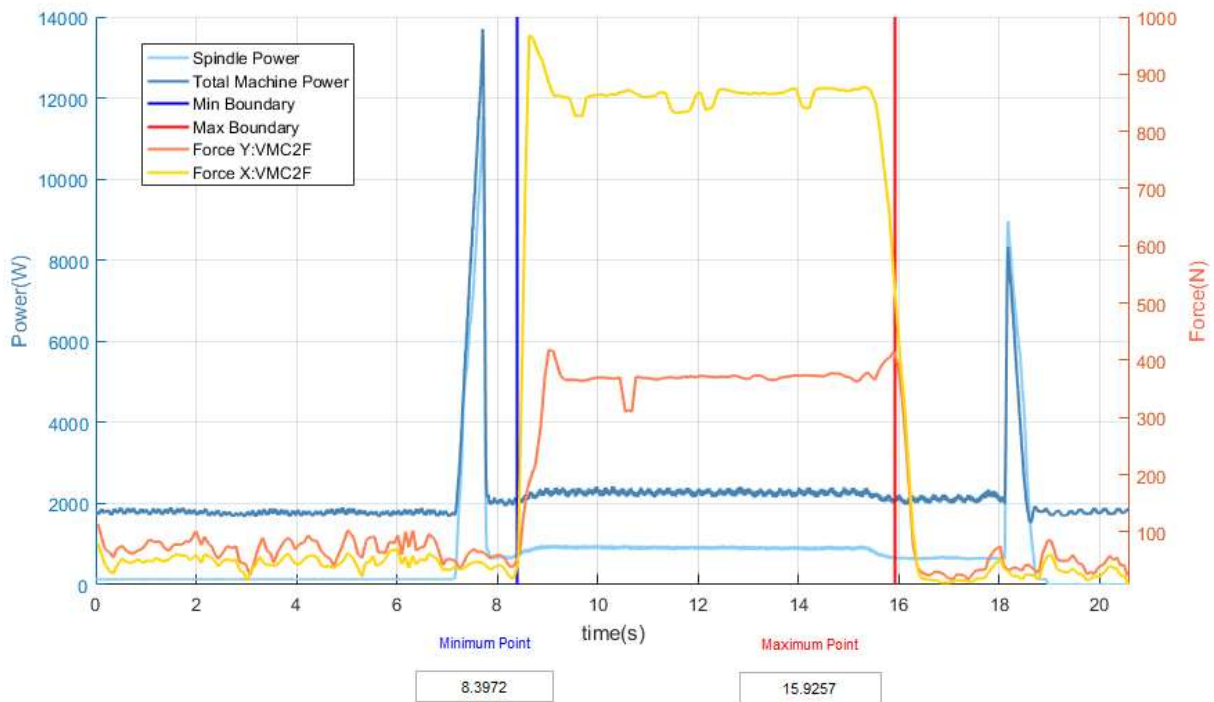


Figure 69. 4 mm depth of cut test, Source: Own contribution

The plots show a very similar behavior as expected. Since the spindle start peaks were very high even though the moving average function was used, the maximum value of power in the plot is too large compared to the power values during the machining. For this reason, it is hard to recognize a high difference in power requirements. The user can click the zoom in option to show only the machining part of the measurement. The calculated data explains better this case. The forces for the 2mm depth case were in the X-axis around 500 N and for the Y axis around half of this value. On the other hand, when the depth was doubled, the forces almost doubled the previous. The cutting forces for the 4mm case were also almost twice the cutting forces for the 2mm case. The machining time was the same and the power consumption for the spindle increased in average 400 Watts. The spindle energy consumption went from 6600 J to 9400 J during the machining. However, the energy consumption of the total machine was very similar.

The most important analysis comes regarding the ECF value because it shows the advantages in energy consumption terms of machining a higher volume. When machining only 2 mm depth, the ECF factor for the total machine is around 40% higher than the 4mm case. However, the cutting forces are almost twice as high and that means a shorter expected life cycle for the tool.

EMCO VMC-600		
Depth of cut	2mm	4mm
Max Force X / N	637	1000
Max Force Y / N	293	440
Max Force Z / N	288	428
Max Force XY / N	638	1003
Machining time (s)	7,52	7,53
Average $F_x$ (N)	90	160
Average $F_y$ (N)	17	27
Fc (N)	499	846
kc (N/mm <sup>2</sup> )	2497	2114
Energy Consumption Spindle	6594	9404
Energy Consumption Total Machine	17080	19774
Average Power Spindle	876	1249
Average Power Total Machine	2270	2627
Peak Power Spindle	19395	19270
Peak Power Total Machine	22678	23247
ECF Spindle	5,513	4,641
ECF Total Machine	14,28	9,759

Table 17. Depth of cut resulting data comparison

### 7.7 Force vs Force

This method allows the comparison between different parameters or two different machine tools. It is interesting to check, what machine needs a higher cutting force for developing the same procedure. It might lead to conclusions like over dimension of the machine.

Figure 70 shows two force tests compared in X and Y axes. Test 1: DMG1F was carried out for a depth of cut  $a_p = 2mm$  and Test2: DMG2F with  $a_p = 4mm$ . It is expected that the forces for a deeper milling are higher.

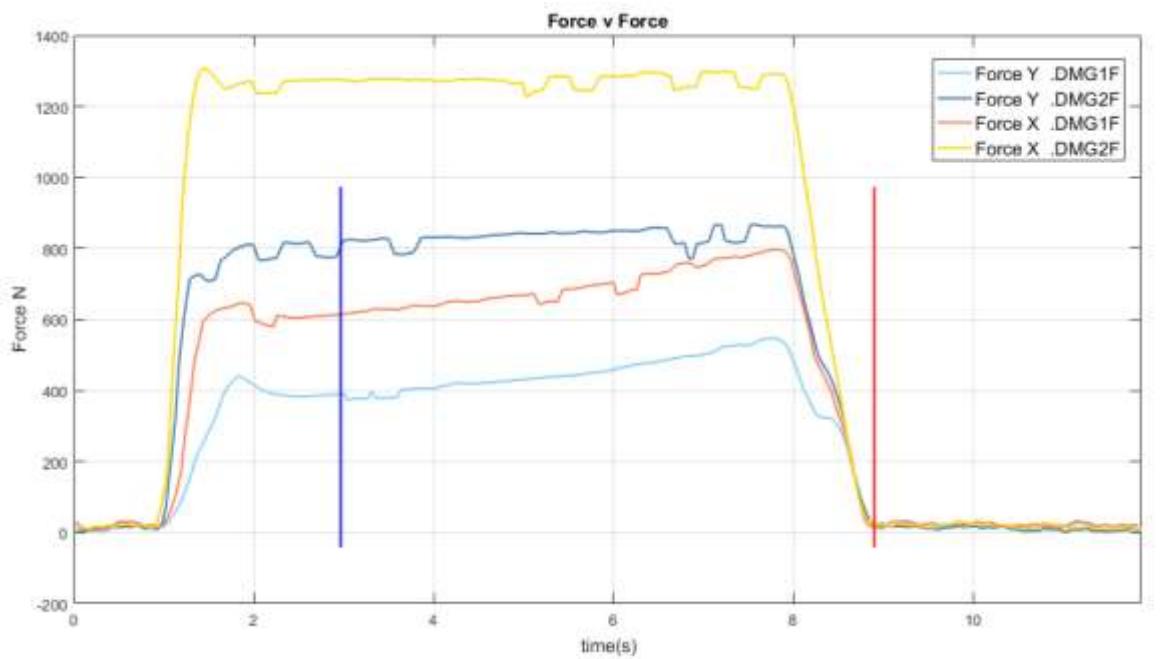


Figure 70. Force X and Y comparison for two different depths of cut (2 and 4 mm), Source: Own contribution

The cutting forces and the cutting power are expected to increase when the depth of cut increases, since these are directly related to the X and Y forces. The oscillations of the power can be attributed to imperfections in the workpiece. For the test 1: DMG1F an increment of the forces over the time is observed. Since this test was the first of the test series done to the workpiece, it is possible that the workpiece was not properly aligned and therefore the depth of cut was slightly increasing.

		DMG1F	DMG2F
Cutting Forces(N)	Average	614.8	1169.6
	Peak	805	1332
Cutting Power (W)		1537	2932.9

Table 18. Cutting Force and Cutting Power of test shown in Figure 70

## 8 Conclusion and Further Outlook

Tools life cycle is basically determined by the force loads they are subject to, if the forces are too high, the amount of necessary tools or inserts needed increases and so do the total costs of the machining process.

As it is not simple to estimate the best solution in terms of total costs, a further analysis that considers tool life and energy costs should be done, in order to find the right machining parameters and machine tools with the highest energy efficiency and the lowest forces possible.

Although the emphasis of the project is the machining process itself, where both force and energy values vary and show interesting results for further analysis. It would also be important to use the software for the comparison of machine tools during a complete cutting operation including the standby time, time for tool change, cutting power, until the machine finishes. The ECF factor would be used to compare energy efficiency and determine the most energy efficient machine tool.

The ECF factor has a potential for machine selection in the industry. If machine tools manufacturers handle out the ECF values of their machines, customers from all the different industrial sectors would easily recognize the most energy efficient machine. First the customers should know their machining requirements, which come from the type of piece, dimension, material and many other factors, but once those basic requirements are known, the machine tool selection process can be done.

There are multiple improvement possibilities for the software. The first one is the implementation of a positioning sensor. This would allow the exact identification of the insert position and the further calculation of the corresponding area and cutting force for each time point. In that manner, the specific force value could be properly calculated and not estimated how it is actually done.

The next improvement possibility is the implementation of the turning and drilling. Machined objects do not only need face-milling but also holes and pieces with different shapes, which are achieved with a combination of many different machining methods. Some calculations have to be implemented to correct the removed volume.

The Dewetron software system available allows the measurement of 12 channels. For this project, only two components have been measured in a parallel manner, but changing the connection points it is possible to reduce the necessary channels per element to 4. This way, one more component could be measured and therefore more information of the process could be evaluated.

The ultrasonic technology is still to be tested at the Institute of Production Engineering. The DMG frequency generator will be replaced and then new measurements will be done.

## List of Illustrations

Figure 1. EU Final energy Consumption by Sector, Source: (European Environment Agency, 2015).....	1
Figure 2. EU Final Energy Consumption of electricity by sector, Source (European Environment Agency, 2015) .....	2
Figure 3. AC Signal example- Instantaneous Voltage, Current and Power, Source: Own contribution.....	5
Figure 4. Active Power with phase shift, Source: Own contribution .....	6
Figure 5. Vector Representation P, Q, S, and $\varphi$ , Source: Own contribution .....	6
Figure 6. Periodical Signal Time Domain Representation, Source: Own contribution .....	8
Figure 7. Periodical Signal Frequency domain Representation, Source: Own contribution....	8
Figure 8. Power Measurement System, Source: Own contribution .....	9
Figure 9. Left: Basic motions in turning operations, Right: Components of the machining, Source: (Astakhov, 2011) .....	11
Figure 10. Cutting Force Components, Source: (Astakhov, 2011) .....	12
Figure 11. Force Contact conditions, Source: (Eberhard, Sven, Marco, & Franz, 2008, p. 215) .....	13
Figure 12. Feed per tooth for milling, Source: (Lacalle, 2011).....	14
Figure 13. Axial and radial depths of cut, Source: (Lacalle, 2011) .....	14
Figure 14. Left: Milling Process and main Parameters, Right: Forces Description, Source: (Berend & Hans Kurt, 2011) .....	14
Figure 15. Piezoelectric Dynamometers. Left: Stationary 3-Component Dynamometer, Right: Longitudinal effect, Source: (KISTLER Group, 2014) .....	16
Figure 16. Measuring Chain for stationary Dynamometer, Source: (KISTLER Group, 2014) .	17
Figure 17. Strain Gauge before and after axial force is applied, Source: Own contribution .	18
Figure 18. Examples of Gages Types: Left: Quarter-Bridge, Center: Middle Bridge, Right: Full Bridge, Source: (National Instruments, 2016).....	18
Figure 19. Spike integration into a machining system, Source: (Promicron, 2016).....	19
Figure 20. 1 Dimension Vibration Assisted Machining, Source: (D.E. Brehl, 2007) .....	21
Figure 21. Tool force comparison between linear VAM and conventional cutting, Source: (D.E. Brehl, 2007).....	22
Figure 22. Machining Strategies for ULTRASONIC 30 linear, Source: (DMG MORI, 2016) ....	23
Figure 23. Dewesoft Recorder, Source: Own contribution .....	25
Figure 24. Cutting Force Data Acquisition, Source: Own contribution .....	26



Figure 25. User Interface for the Force Data Evaluation, Source: (Grabner, 2016).....	27
Figure 26. Initial Modification to the Force Interface, Source: Own contribution .....	28
Figure 27. Initial Appearance of the Interface and selection of new type of comparison, Source: Own contribution .....	29
Figure 28. Data Upload for Force vs Power Comparison, Source: Own contribution .....	29
Figure 29. Power Variables renaming, Source: Own contribution .....	31
Figure 30. Machining Process relevant data, Source: Own contribution .....	31
Figure 31. Table with cutting process parameters and other relevant data, Source: Own contribution.....	32
Figure 32. Geometry in face milling: Process angle determination, Source: (Heikkala, 1995, p. 5).....	34
Figure 33. Plotting of independent force data and selection of start of machining, Source: Own contribution .....	36
Figure 34. Force vs Force Interface, Source: Own contribution .....	37
Figure 35. Power profile of a multi-pass CNC milling, Source (Li, Chen, Tang, & Li, 2016, p. 3) .....	38
Figure 36. Power profile of a single-pass CNC milling, Source. Own contribution .....	38
Figure 37. Equivalent Circuit Diagram of the Power Measurement .....	40
Figure 38. Frequency Spectrum for Spindle Voltage (SF:10kHz), Source: Own contribution	41
Figure 39. Spindle Voltage Time domain (SF: 10 kHz), Source: Own contribution .....	41
Figure 40. Spindle Voltage Time domain (SF: 200 kHz), Source: Own contribution .....	42
Figure 41. Frequency Spectrum for Spindle Voltage (SF:200kHz), Source: Own contribution .....	42
Figure 42. Power measured at different sampling rates, Source: Own contribution.....	43
Figure 43. Channels Set-Up for the DEWESOFT Software. 12 Channels, 20 kHz Sampling frequency, Source: Own contribution.....	44
Figure 44. Left: Voltage channel configuration, Right: Current channel configuration, Source: Own contribution .....	44
Figure 45. Up and Down milling, Source: Own contribution .....	45
Figure 46. Left: Time Curve of Forces for a full slot test, Right: Cutting Force at a specific angle $\varphi$ , Source: (Grabner, 2016) .....	46
Figure 47. $F_c, F_x, F_y$ : One Tooth, VMC 600 Machine, $ae=25$ mm, $ap=5$ mm, Full Slot.....	46
Figure 48. Difference (in Percentage) Between $F_c$ and $F_x, F_y$ .....	47
Figure 49. $F_c, F_x, F_y$ : One Tooth, VMC 600 Machine, $ae:16$ mm, $ap: 3$ mm, Full Slot.....	47

---

Figure 50. One Tooth Difference (in Percentage) Between $F_c$ and $F_x, F_y$ .....	48
Figure 51. Forces diagram and angle $\varphi$ , Source: Own contribution.....	49
Figure 52. Chip thickness (left), specific force (middle), and cutting force (right) for one tooth climb- milling, Source (Eberhard, Sven, Marco, & Franz, 2008, p. 215) .....	50
Figure 53. Forces in X and Y axis and cutting force $F_c$ for a 50% overlap climb-milling, Source: (Grabner, 2016) .....	50
Figure 54. 10% overlap. Climb-milling, Source: Own contribution .....	51
Figure 55. 75% Overlap. Climb-milling, Source: Own contribution .....	51
Figure 56. 25% overlap. Climb-milling, Source: Own contribution .....	52
Figure 57. Specific Cutting Force and Cutting depth for steel, Source (Berend & Hans Kurt, 2011, p. 55).....	53
Figure 58. ISO 90P Source: (BOEHLERIT, 2016) .....	55
Figure 59. Milled workpiece with different depths of cut, Source: Own contribution .....	57
Figure 60. Left: DMU Setup, Right: EMCO VMC600 Milling Setup, Source: Own contribution. ....	57
Figure 61. Power and Force typical plot for milling .....	58
Figure 62. DMG MORI Force and Power Milling .....	59
Figure 63. EMCO VMC600 Force and Power Milling.....	60
Figure 64. 20% overlap force and power plot, Source: Own contribution .....	61
Figure 65. 50% Overlap force and power plot Source: Own contribution.....	62
Figure 66 . One tooth 4 mm Depth of cut DMG, Source: Own contribution.....	63
Figure 67. Two teeth, 4mm depth of cut, Source: Own contribution .....	64
Figure 68. 2 mm depth of cut test, Source: Own contribution .....	66
Figure 69. 4 mm depth of cut test, Source: Own contribution .....	67
Figure 70. Force X and Y comparison for two different depths of cut (2 and 4 mm), Source: Own contribution .....	69

## List of Tables

Table 1. Technical Data Dewetron Acquisition System, Source: (DEWETRON Elektronische Messgeraete Ges. m.n.H., 2012) .....	10
Table 2. Measurement Chain Equipment Reference (KISTLER + National Instruments).....	17
Table 3. Technical Data SPIKE measurement system. ....	19
Table 4. Properties of the cutting test for a Power sampling rate of 200kHz .....	43
Table 5. Differences in the power and energy calculations for SF=200kHz, 50kHz and 20kHz .....	43
Table 6. Opposite direction full slot milling tests to determine angle $\varphi$ when $F_y = -F_x$ .	48
Table 7. Relevant further test parameters for $kc$ tests .....	48
Table 8. Technical Data of the machine tools, Source (EMCO MAIER GmbH, 1998), (SAUER GmbH, 2015) .....	54
Table 9. OSAWA mill relevant data .....	55
Table 10. 16 mm Mill relevant data .....	55
Table 11. Boehlerit Mill 16 mm relevant data .....	55
Table 12. Full Slot measurements parameters .....	56
Table 13. Different machine tools measurement parameters .....	56
Table 14. Relevant data for machine tool comparison .....	60
Table 15. Relevant data for cut width comparison .....	62
Table 16. Most Relevant data for number of teeth test comparison .....	64
Table 17. Depth of cut resulting data comparison.....	68
Table 18. Cutting Force and Cutting Power of test shown in Figure 70 .....	69

## Bibliography

**Astakhov, Viktor P. 2011.** Turning. [book auth.] LaCalle Astakhov. *Modern Machining Technology*. s.l. : Woodhead Publishing, 2011, pp. 1-78.

**Berend, Denkena and Hans Kurt, Tönshoff. 2011.** *Spanen Grundlagen*. Heidelberg : Springer, 2011.

**Brehl, D.E and Dow, T.A. 2007.** Review of vibration-assisted machining. 2007, pp. 153-172.

**CECIMO. 2016.** CECIMO PRESS RELEASE. [Online] June 22, 2016. [Cited: August 22, 2016.] [http://www.cecimo.eu/site/fileadmin/Press\\_releases/CECIMO\\_press\\_release\\_22062016.pdf](http://www.cecimo.eu/site/fileadmin/Press_releases/CECIMO_press_release_22062016.pdf).

**Dahmus, J.B and T.G, Gutowski. 2004.** An environmental analysis of machining. 2004, pp. 643-652.

**Davim, J. Paulo. 2011.** Preface: Modern Machining Technology. [book auth.] Viktor P. Astakhov, et al. *Modern Machining Technology*. Cambridge : Woodhead Publishing, 2011, p. 372.

**DEWETRON. 2016.** DEWETRON CHASSIS DEWE 30. *DEWETRON Devices*. [Online] May 2016. [Cited: August 11, 2016.] [http://www.dewetron.com/wp-content/uploads/2016/05/dewetron\\_dewe-30\\_chassis\\_e.pdf](http://www.dewetron.com/wp-content/uploads/2016/05/dewetron_dewe-30_chassis_e.pdf).

**DEWETRON Elektronische Messgeraete Ges. m.n.H. 2012.** *DEWETRON Technical Reference Manual*. Graz, Austria : DEWETRON GmbH, 2012.

**DMG MORI. 2016.** Ultrasonic Linear 30 . *DMG MORI Products*. [Online] October 26, 2016. <http://us.dmgmori.com/blob/127642/1c610ae40a50b3f29bc39108f3a0754f/pu0uk-ultrasonic-pdf-data.pdf>.

**Eberhard, Paucksch, et al. 2008.** *Zerspantechnik*. Wiesbaden, Germany : Vieweg Teubner, 2008.

**EMCO MAIER GmbH. 1998.** *User Hanbook EMCO VMC 600 D*. Hallein, Austria : EMCO, 1998.

**European Comission. 2016.** Energy 2020. *European Comission*. [Online] August 11, 2016. [https://ec.europa.eu/energy/sites/ener/files/documents/2011\\_energy2020\\_en\\_0.pdf](https://ec.europa.eu/energy/sites/ener/files/documents/2011_energy2020_en_0.pdf).

**European Environment Agency. 2015.** Final Energy Consumption by sector and Fuel. *European Environment Agency*. [Online] International Energy Agency, Statistical Office of the European Union (Eurostat), August 31, 2015. [Cited: August 19, 2016.] <http://www.eea.europa.eu/data-and-maps/indicators/final-energy-consumption-by-sector-9/assessment>.

**Grabner, Ewald. 2016.** Force Data Acquisition Software NI-DAQ. Force Data Analysis Software (BOF). *NI-DAQ, BOF*. Institute of Production Engineering, Graz, Austria : IFT, April 2016.

**Heikkala, J. 1995.** Determining of cutting-force components in face-milling. *Journal of Material Processing Technology*. 1995, pp. 1-8.

**KISTLER Group. 2014.** Cutting Force Measurement. *KISTLER*. [Online] May 1, 2014. <https://www.kistler.com/?type=669&fid=65&model=download>.

**Lacalle, L. Norberto López de. 2011.** Milling: Modern Machining Technology. *Modern Machining Technology*. Cambridge : s.n., 2011, pp. 213-234.

**Li, Congbo, et al. 2016.** Selection of optimum parameters in multi-pass face milling for maximum energy efficiency and minimum production cost. *Journal of Cleaner Production*. 2016, pp. 1-14.

**Maurotto and Wickramarachchi, C.T. 2015.** Experimental investigations of effects of frequency in ultrasonically-assisted end-milling of AISI 316L: A feasibility study. *ScienceDirect*. October 19, 2015, p. 8.

**National Instruments. 2016.** Measuring Strain with Strain Gages. *National Instruments Whitepapers*. [Online] September 26, 2016. <http://www.ni.com/white-paper/3642/en/#toc2>.

**Oppenheim, Alan V. and Schafer, Ronald W. 2010.** Sampling of Continuous-Time Signals. [book auth.] Alan V. Oppenheim and Ronald W. Schafer. *Discrete-Time Signal Processing*. Upper Saddle River, NJ 07458 : Pearson, 2010, pp. 153-155.

**Oppenheim, Alan V. 2014.** *Signals and Systems*. Edinburgh : PrenticeHall, 2014.

**Paetzold, J. 2011.** Messung elektrischer Energie - Grundlagen und Erfahrung. [Buchverf.] Technische Universität Chemnitz. *Methoden der energetisch-wirtschaftlichen Bilanzierung und Bewertung in der Produktionstechnik*. 2011, S. 19.

**Promicron. 2016.** SPIKE, Sensory tool holder. *Spike Product Portfolio*. [Online] September 26, 2016. [http://www.pro-micron.de/fileadmin/user\\_upload/Bilder/Produkte/SPIKE\\_-\\_Sensorischer\\_Werkzeughalter/Aktualisierung\\_Produktuebersicht/SPIKE-1\\_1-Productinformation\\_engl-internet.pdf](http://www.pro-micron.de/fileadmin/user_upload/Bilder/Produkte/SPIKE_-_Sensorischer_Werkzeughalter/Aktualisierung_Produktuebersicht/SPIKE-1_1-Productinformation_engl-internet.pdf).

**SAUER GmbH. 2015.** *ULTRASONIC 30 Linear Operating Manual*. Stipshausen, Germany : SAUER, 2015.

**Silberschmidt, Vadim V., Mahdy, Sameh M. A. and Gouda, Moustafa A. 2014.** Surface-roughness Improvement in Ultrasonically Assisted Turning. *ScienceDirect*. 2014, p. 6.

**Tektronix. 2013.** Fundamental of AC Power Measurements. *Tektronix Documents*. [Online] December 2, 2013. [Cited: August 17, 2016.] <http://info.tek.com/www-fundamentals-of-ac-power-measurements.html>.

**THOE, T.B, ASPINWALL, D.K and WISE, M. L. H. 1997.** Review on ultrasonic machining. 1997, pp. 1-17.

**Zein, André. 2012.** *Transition Towards energy Efficient Machine Tools*. Berlin : Springer-Verlag, 2012.

Appendix

G2 - General purpose

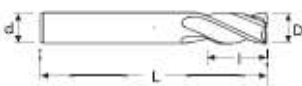


GB405 - G2C54

Ø mm	-6	6.5-12	13-20
tol. D µ	0 / -20	0 / -25	0 / -30

G2410 - G2411 - G2412 - G2413

Ø mm	-6	6.5-12	13-20
tol. D µ	0 / -30	0 / -35	0 / -40



MG	MG	MG	MG	MG	MG
BB	FW20	FW20	FW20	FW20	FW20
N	N	N	N	N	N

D	d	l	L	Stock	Stock	Stock	Stock	Stock	Stock
mm 1	4	3	50	●	●				
1.5	4	4.5	50	●	●				
2	4	6	50	●	●				
2	4	9	75			●			
2.5	4	7	50		●				
3	4	8	50	●	●				
3	4	15	75			●			
3.5	4	10	50		●				
4	4	11	50	●	●				
4	4	20	75			●			
4.5	6	13	50		●				
5	6	13	50	●	●				
5	6	25	75			●			
5	6	30	100				●		
5.5	6	13	50		●				
6	6	15	50	●	●				
6	6	25	75			●			
6	6	30	100				●		
6.5	8	17	60		●				
7	8	17	60		●				
7	8	35	100				○		
7.5	8	17	60		●				
8	8	20	60	●	●				
8	8	35	100				●		
8	8	40	150					●	
8.5	10	23	75		●				
9	10	23	75		●				
9	10	40	100				○		
10	10	30	75	●	●				
10	10	40	100				●		
10	10	50	150					●	
10.5	12	25	75		●				
11	12	28	75		●				
11	12	45	100				○		
12	12	30	75	●	●				
12	12	45	100					●	

● stock standard ○ non-standard stock ■ stock exhaustion

Appendix 1. Mill for testing



GB405 - G2CS4			
Ø mm	~6	6.5-12	13-20
tol. D µ	0 / -20	0 / -25	0 / -30

G2410 - G2411 - G2412 - G2413			
Ø mm	~6	6.5-12	13-20
tol. D µ	0 / -30	0 / -35	0 / -40



	MG	MG	MG	MG	MG	MG			
	HR	PCBN	PCBN	PCBN	PCBN	PCBN			
	N	N	N	N	N	N			
D	d	l	L	Stock	Stock	Stock	Stock	Stock	Stock
mm 12	12	50	150						
14	14	26	83		●				●
16	16	32	92		●				
16	16	70	150						●
16	16	40	200						●
18	20	40	100		●				
18	20	80	150						○
20	20	40	100		●				
20	20	80	150						●
20	20	40	200						●

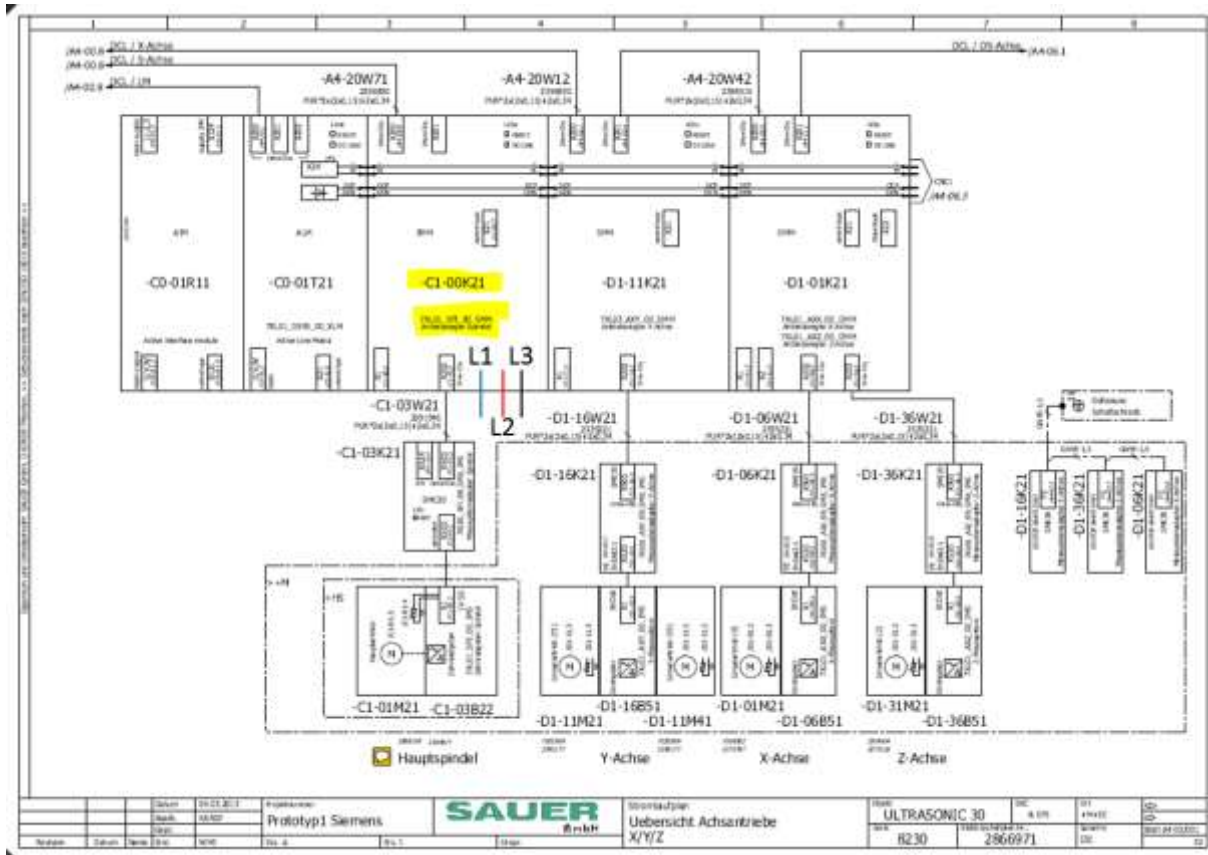
● stock standard ○ non-standard stock ■ stock reduction



Single Motor Modules in booksize format						
Technical specifications (continued)						
DC link voltage 230 ... 230 V DC	Single Motor Module in booksize format					
Internal air cooling	6SL3120-...	TTE24-SAA3	TTE25-SAA3	TTE26-SAA3	TTE27-SAA3	TTE32-GAA4
External air cooling	6SL3121-...	TTE24-SAA3	TTE25-SAA3	TTE26-SAA3	TTE27-SAA3	TTE32-GAA4
Cold plate cooling	6SL3126-...	TTE24-SAA3	TTE25-SAA3	TTE26-SAA3	TTE27-SAA3	TTE32-GAA4
Liquid cooling	6SL3125-...	-	-	-	-	TTE32-GAA4
<b>Output current</b>						
• Rated current $I_{rated}$	A	45	60	85	132 (105 <sup>1)</sup>	200 (140 <sup>1)</sup>
• Base-load current $I_b$	A	35	52	65	105 (54)	147 (99)
• For 50 duty $I_{50}$ (40%)	A	90	90	110	150 (120)	230 (181)
• $I_{max}$	A	85	113	141	210	282
<b>Rated pulse frequency</b>	KHz	4	4	4	4	4
• <b>Type rating<sup>2)</sup></b>						
• Based on $I_{rated}$	kW (HP)	24 (30)	32 (40)	48 (60)	71 (100)	107 (150)
• Based on $I_b$	kW (HP)	21 (28)	28 (40)	37 (50)	57 (75)	78 (100)
<b>DC link current <math>I_d</math><sup>3)</sup></b>	A	54	72	102	158	200
<b>Current carrying capacity</b>						
• DC link busbars	A	200	200	200	200	200
• 24 V DC busbars	A	20	20	20	20	20
If, due to a number of Line and Motor Modules being mounted side-by-side, the current carrying capacity exceeds 20 A, an additional 24 V DC connection using a 24 V terminal adapter is required (max. cross-section 6 mm <sup>2</sup> , max. fuse protection 20 A)						
<b>DC link capacitance</b>	$\mu$ F	1175	1410	1660	2620	3065
<b>Current requirement At 24 V DC, max.</b>	A	1.2	1.2	1.5	1.5	1.5
<b>Internal/external air cooling</b>						
• <b>Power loss<sup>4)</sup></b>						
- Maximum power loss with internal air cooling in control cabinet	kW	0.45	0.62	0.79	1.28	2.09
- Typical losses with internal air cooling in control cabinet <sup>5)</sup>	kW	0.38	0.55	0.77	1.28	2.02
- With external air cooling, int. fan <sup>6)</sup>	kW	0.14/0.32	0.16/0.48	0.21/0.59	0.28/1.0	0.47/1.62
• <b>Cooling air requirement</b>	m <sup>3</sup> /s (ft <sup>3</sup> /s)	0.031 (1.095)	0.031 (1.095)	0.044 (1.554)	0.144 (5.085)	0.144 (5.085)
• <b>Sound pressure level <math>L_{pA}</math> (1 m)</b>	dB	< 65	< 65	< 60	< 73	< 73
<b>Cold plate cooling</b>						
• <b>Power loss, int. fan<sup>6)</sup></b>	kW	0.11/0.34	0.13/0.48	0.15/0.62	0.24/1.05	0.39/1.7
• <b>Thermal resistance <math>R_{th}</math></b>	K/W	0.055	0.055	0.05	0.028	0.028

Appendix 2. DMG MORI Spindle Motor Module Specifications

# Appendix



Appendix 3. Spindle Physical Connection for Power Measurements